The Pluto-Charon system as revealed during the mutual events.

THE PLUTO–CHARON SYSTEM AS REVEALED DURING THE MUTUAL EVENTS

by

Robert Louis Marcialis

A Dissertation Submitted to the Faculty of the
DEPARTMENT OF PLANETARY SCIENCES
In Partial Fulfillment of the Requirements
For the Degree of
DOCTOR OF PHILOSOPHY
In the Graduate College
THE UNIVERSITY OF ARIZONA

1 9 9 0

Order Number 9024512

The Pluto-Charon system as revealed during the mutual events

Marcialis, Robert Louis, Ph.D.

The University of Arizona, 1990

U·M·I
300 N. Zeeb Rd.
Ann Arbor, MI 48106

THE PLUTO–CHARON SYSTEM AS REVEALED DURING THE MUTUAL EVENTS

by

Robert Louis Marcialis

A Dissertation Submitted to the Faculty of the
DEPARTMENT OF PLANETARY SCIENCES
In Partial Fulfillment of the Requirements
For the Degree of
DOCTOR OF PHILOSOPHY
In the Graduate College
THE UNIVERSITY OF ARIZONA

1 9 9 0

THE UNIVERSITY OF ARIZONA
GRADUATE COLLEGE

As members of the Final Examination Committee, we certify that we have read the dissertation prepared by Robert Louis Marcialis

entitled The Pluto-Charon System as Revealed During the Mutual Events

and recommend that it be accepted as fulfilling the dissertation requirement for the Degree of Doctor of Philosophy.

William B. Hubbard — Date 2/16/90

Date 2/16/90

Date 2-16-90

Date 16 Feb 90

Date 2/16/90

Final approval and acceptance of this dissertation is contingent upon the candidate's submission of the final copy of the dissertation to the Graduate College.

I hereby certify that I have read this dissertation prepared under my direction and recommend that it be accepted as fulfilling the dissertation requirement.

William B. Hubbard
Dissertation Director — Date 2/16/90

STATEMENT BY AUTHOR

This dissertation has been submitted in partial fulfillment of requirements for an advanced degree at The University of Arizona and is deposited in the University Library to be made available to borrowers under rules of the Library.

Brief quotations from this dissertation are allowable without special permission, provided that accurate acknowledgement of source is made. Requests for permission for extended quotation from or reproduction of this manuscript in whole or in part may be granted by the copyright holder.

SIGNED: Robert L. Marcialis

TABLE OF CONTENTS

LIST OF ILLUSTRATIONS

LIST OF TABLES

ABSTRACT

This year is the last of a five-year interval when the Earth passes through the orbital plane of Pluto and its satellite Charon, causing alternate transits and occultations of the satellite as seen from Earth. Spectrophotometric observations of the system made both in and out of eclipse have been obtained in the visual and near-infrared. The Pluto–Charon system is found to be compositionally diverse, a result unanticipated before the mutual events. Water frost has been identified and is ubiquitous on Charon's surface, while Pluto has a methane veneer. The spectral activity of Pluto's methane is seen to vary with rotational phase, *i.e.*, planetary longitude. On Pluto, composition appears to be correlated with surface albedo. Dark regions tend to be redder and depleted in methane relative to bright regions. Dependence of geometric albedo with wavelength has been calculated for both bodies, from 0.4 to 2.4 μm. The albedo model of Marcialis (1983, 1988) has emerged favorably after several severe tests.

Accurate radii and system bulk density derived from the mutual events have been used to construct models of phenomena unanticipated a decade ago. Charon's gravity is feeble enough that it could have shed a substantial primordial methane inventory to space and to Pluto, thereby explaining its different surface composition and lower albedo. Recent interior models are used to show that viscous relaxation of topography is expected to be significant on Pluto but not on Charon. Horizontal topographic features on the primary probably are limited in extent to less than a few tens of kilometers (or are geologically young), much as has been found subsequently for Triton. Globally, Pluto's figure is essentially hydrostatic.

Astrometric observations of the system are presented, as is evidence that the discovery of Charon just seven years before the initial mutual events was not fortuitous, but most probable. The astrometry will help to refine Pluto's orbit, making prediction of future stellar occultations by the system more reliable.

CHAPTER 1

INTRODUCTION

In the half century following Clyde Tombaugh's 1930 discovery of Pluto, learning anything substantial about the ninth planet proved to be one of the more difficult tasks of planetary astronomy. The rotational period ($6^{d}.4$) was determined by Walker and Hardie (1955), and low-resolution filter photometry gave the first clues about the surface composition of the planet (Cruikshank *et al.* 1976, 1977; Lebofsky *et al.* 1979). However, Pluto remained largely inaccessible as a planetary laboratory. Most Hadean research centered on astrometry, in the hope that a refined orbital determination would allow observation of mutual perturbations between Uranus, Neptune, and Pluto. If these perturbations could be measured, then an estimate of Pluto's mass could be derived. Radius estimates were derived simply from broadband photometry and constraining the albedo to be less than unity. The young disciplines of thermal modelling and speckle interferometry seemed our best hopes for refining the radius estimate.

Positional measurements obtained at the A. J. Dyer Observatory and reduced at the USNO comprise Chapter 7 of this document.

As a by-product of the astrometry program to refine Pluto's orbit determination, Christy and Harrington discovered in 1978 that several of the highest quality images of Pluto were out-of-round. Yet on the same plates images of nearby stars retained their symmetry. Pluto had a satellite, which Christy named Charon (after the mythological character who ferried the souls of the dead across the river Styx into Hades). The discovery of Charon has proven to be a crack in the dam which allows us to sample some of the waters of the Styx. A flood of information, both theoretical and observational, has been wrung from the meager supply of photons which Pluto redirects toward Earth. Kepler's Third Law gave one immediate result—a much better mass estimate of the system.

I recall with some fondness my first original scientific thought: If Pluto had a satellite, then there must be two times per orbit around the Sun when the Earth transects the Pluto–Charon orbital plane. Off I went to see John Lewis, whom I wanted to be the first to hear of my "discovery." My elation soon subsided, rather catastrophically, with the realization that such a configuration could exist for only two brief periods every 248 years. What were the chances it would occur in my lifetime? Taking some consolation in the fact that I had not embarrassed myself in front of Professor Lewis, I returned to my dormitory room. My roommates were nonplussed, but the seed had been planted.

Leif Andersson was having similar ideas (1978). Based upon the orbit of the satellite, he showed that one of these special times of alignment (termed mutual event season) either had just finished, or was just about to begin. By timing the duration of alternate satellite passages behind (occultation) and in front of (transit) the primary, it would be possible to deduce the radii of both Pluto and Charon to within something like 10 km. The close coincidence between satellite discovery and onset of mutual events seemed amazingly fortuitous. However, Chapter 8 of this dissertation shows that very little luck was involved.

While a Master's student at Vanderbilt University, I realized from collaboration with Douglas Hall on *RS Canum Venaticorum* binary stars that the out-of-eclipse lightcurve slope had to be modelled out of mutual event observations in order to invert a light curve for the albedo distribution. Meanwhile, Robert Hardie had challenged me to explain the observed evolution of Pluto's light curve over the preceding 35 years. The result of 1 1/2 years' effort was a model of the surface albedo distribution of Pluto which was consistent with the observations (Marcialis 1983, 1988*a*). This model calls for two dark equatorial regions to modulate the rotational light curve, but requires two very bright polar caps and/or bright surface frosts which sublime to explain the marked dimming in mean light level observed from year to year. One reason early radius determinations by speckle interferometry were so inaccurate was that the observations were made almost exactly at minimum light (Bonneau and Foy 1980). At this time Pluto presents a very nonuniform albedo distribution.

Although onset of the events was imminent, Charon's orbit was not determined precisely enough to know *when* (within a 6–10 hour stretch) they would occur. At the 1983 meeting of the American Astronomical Society's Division for Planetary Sciences, the inaugural meeting of the Pluto–Charon Mutual Eclipse Season Campaign (PCMESC) was convened, largely through the efforts of Edward Tedesco. An immediate goal of the PCMESC was to coordinate searches of Pluto's light curve for mutual events. Once event detection began, the PCMESC was to provide a vehicle for planning experiments, to encourage collaboration of observers, to archive data, and to establish a newsletter, *The Ninth Planet News*.

As total events were predicted to be about six hours in duration, no single telescope could possibly monitor an entire event at low airmass. Since several sites were needed, standardization of comparison stars and observing techniques were essential to achieve maximum benefit. An example collaboration of PCMESC members appears as Chapter 5, in which the separate albedos of Pluto and Charon were determined as a function of wavelength.

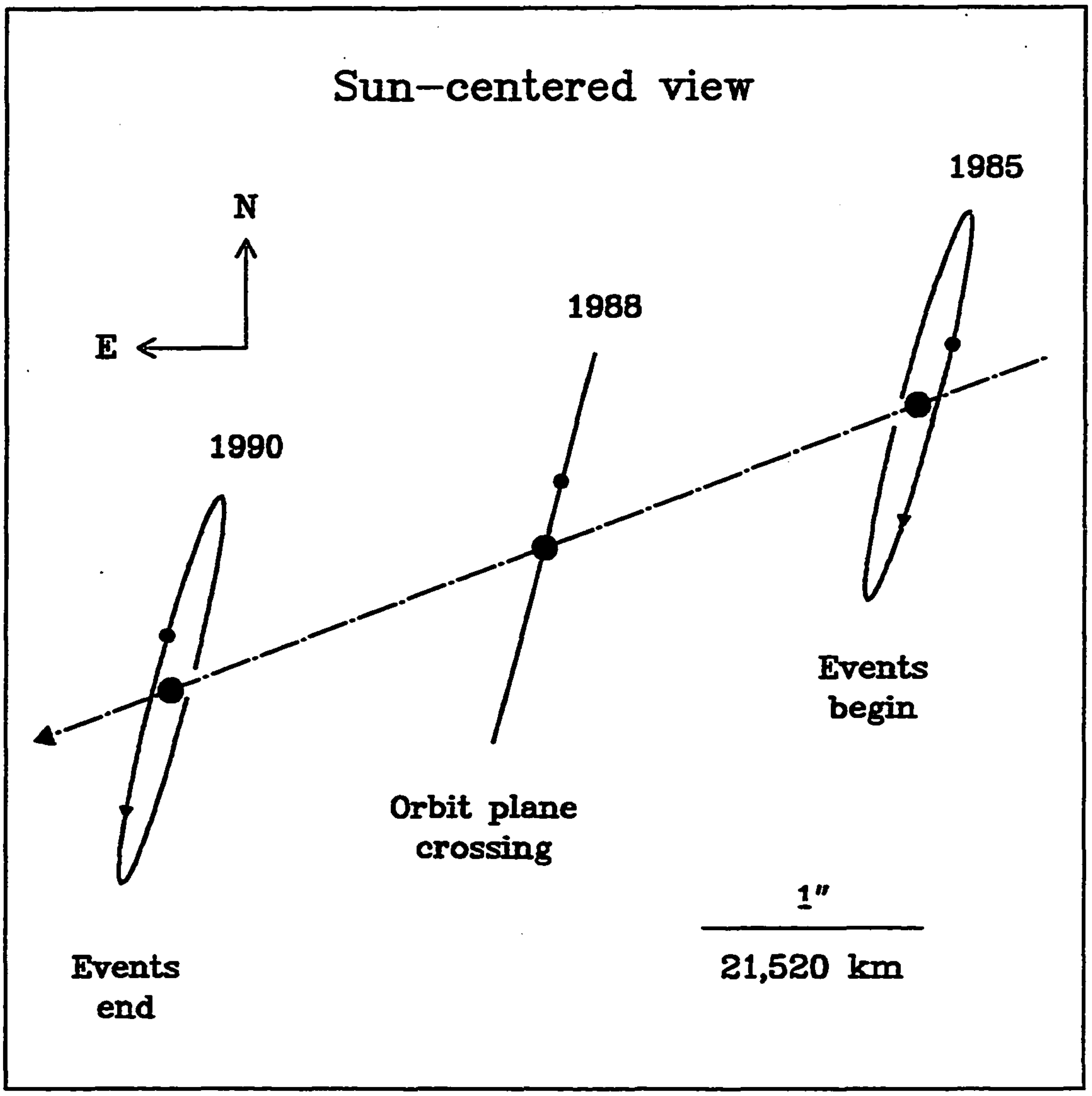

Figure 1.1. Viewing geometry for the Pluto–Charon mutual event season, 1985–1990. The system advances about 15° along its orbit about the Sun over the course of the event season. Adapted from Beatty (1985).

Systematic photometric observations of Pluto were initiated by several groups (Binzel and Mulholland 1983, 1984; Tholen and Tedesco 1984). Along with Marc Buie and Uwe Fink, one of my first observing projects at the University of Arizona was an unsuccessful search for events. Finally, the long-awaited positive detections of the first partial events came in early 1985 (Binzel *et al.* 1985). As projected onto the sky plane, the geometry of the mutual events is depicted in Figure 1.1.

To date, the best models of mutual events to extract system parameters (radii, bulk density, and the specifics of Charon's orbit) have been constructed by David Tholen, Richard Binzel, and Marc Buie (*cf.* Binzel *et al.* 1985; Binzel 1988; Tholen 1987, 1989; Tholen *et al.* 1987, Tholen and Buie 1989). Annual papers by Tholen and coauthors (Tholen *et al.* 1987*a,b*, Tholen and Buie 1988) have been useful for announcing the circumstances of the events, and declaring which comparison stars should be used.

Over the past five years, both Edward Tedesco and I have gathered data sets of mutual event observations which thus far have not been folded into the solution. Together our database comprises a substantial fraction of all observations, second only to Tholen's. Unfortunately, reduction of the data could not be accomplished in time for inclusion here. Analysis of these data will occupy my time over the next few years, and will serve as both a check and an augmentation of previously published results by others.

The bulk of this document is aimed more toward the goal of discerning the separate compositions of Pluto and Charon, rather than their geometry. Most observations were conducted in the near-infrared region of the spectrum. Before the events, it was assumed out of sheer ignorance that planet and satellite had identical compositions and histories. The picture which emerges from the current research is that their surfaces are very different in their chemical ingredients and, very likely, in geological histories and cratering records as well. Charon's surface is typical of water frost, while Pluto's shows only methane absorptions. Out-of-eclipse observations reported here show the spectral activity of methane to be variable with rotational phase on Pluto. It is demonstrated that the surface of Pluto itself has a pronounced inhomogeneity in makeup, with regions bright in the visual seemingly methane-enriched. Since the dark areas have persisted for nearly 40 years, further demands can be made on global models of seasonal methane migration.

To explain the global difference in surface constitutions, a model of atmospheric escape from Charon is presented. To explain the compositional dichotomy, there is no need to form the satellite by blasting Pluto with a large impactor; results of the calculation are consistent with the observations. New interior models of Pluto made possible by mutual event observations estimate that methane comprises the outer 10–30 km of Pluto's "crust" (Simonelli and Reynolds 1989, McKinnon and Mueller 1988). Chapter 6 details the first attempt to address methane rheology. The viscous relaxation model concludes that no topography of horizontal extent more than a few tens of kilometers can persist on Pluto over the age of the solar system, and implies that more advanced viscoelastic models are worthy of consideration.

It is the intent of this dissertation to demonstrate the wide diversity of investigations made possible by the mutual events, and to synthesize them into our grand picture of the workings of what will soon regain its title as the solar system's outermost known planet. The realm of Hades has turned into one of the most interesting laboratories in our planetary system.

CHAPTER 2

THE SURFACE COMPOSITION OF CHARON: TENTATIVE IDENTIFICATION OF WATER ICE

The 3 March 1987 Charon occultation by Pluto was observed in the infrared at 1.5, 1.7, 2.0, and 2.35 micrometers. Subtraction of fluxes measured between second and third contacts from measurements made before and after the event has yielded, for the first time, individual spectral signatures for each body at these wavelengths. Charon's surface appears extremely depleted in methane relative to Pluto. Constancy of flux at 2.0 micrometers throughout the event shows that Charon is effectively black at this wavelength, which is centered on a very strong water absorption band. Thus, the measurements suggest the existence of water ice on Pluto's moon.

2.1. Introduction

The current season of mutual events between Pluto and its satellite Charon presents the opportunity for many unique experiments. For example, monitoring of these events allows the determination of absolute sizes and bulk density for these bodies to unprecedented precision. It is also possible to separate the contributions of both bodies to the total light.

Total occultations of the satellite permit Pluto to be observed uncontaminated by light from Charon. A spectrum obtained during totality may be subtracted from the mean of spectra obtained just before and just after an event. The remainder is a spectrum of the Pluto-facing hemisphere of Charon alone. Both bodies rotate synchronously, which during a central event amounts to only about 2°. Any color variation therefore must arise from compositional differences between the two bodies, rather than a regional variation on the surface of an individual body.

Near-infrared spectrophotometry is a powerful diagnostic tool for the identification of ices on outer solar system bodies because of the strength of molecular transitions in the 1.0 to 2.5 μm region. Based on elemental abundances and the stability of these frosts, the candidate materials for solid surfaces are relatively few, and even filter photometry in the 1.0 to 2.5 μm region is highly diagnostic of surface composition. We report here observations of an occultation of Charon by Pluto with a near-infrared filter set selected to distinguish the most likely surface constituents.

2.2. Observations

The observations reported here were made with the Infrared Photometer and the Multiple Mirror Telescope Observatory (MMTO) at Mt. Hopkins, Arizona. This photometer uses an InSb detector cooled with liquid helium. Measurements were made through an aperture of 8.7″ diameter, and relative to sky reference areas 10″ above and below Pluto in elevation. The stars SAO 120107, HD 105601, and HD 129655 were used for absolute flux calibration.

Data on Pluto were recorded between 0730 and 1315 UT on 1987 March 03. The approximate geometry of the Pluto–Charon system for these times is indicated in Figure 2.1. According to the ephemeris of Tholen (personal communication), this interval spanned the times from roughly one hour before first contact until mere minutes preceding fourth contact. Observations were terminated at approximately 1315 due to brightening of the sky. Skies were clear all night, with temperatures within

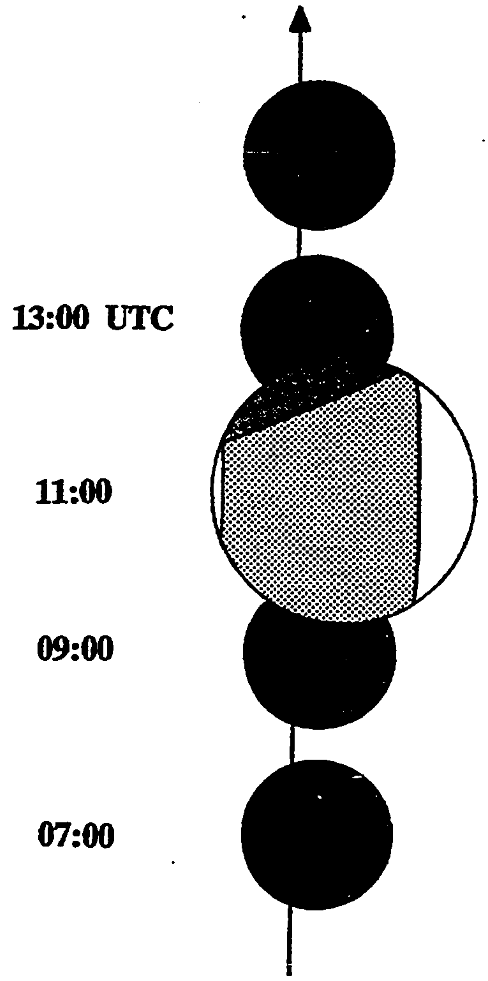

Figure 2.1. Approximate geometry of the 3 March 1987 occultation of Charon by Pluto. The satellite was completely hidden for about two hours.

a couple of degrees of freezing. Seeing was about 1″ for the entire night, with the exception of about an hour from 0930 to 1030, when it degraded to about 2″.

Because of the faintness of Pluto, it is currently impossible to obtain a continuous infrared spectrum of Pluto at reasonable signal-to-noise during the few short hours of a single eclipse event. We therefore observed with four filters, each of which has a spectral resolution of about 5%, or 0.1 μm (*cf.* MMTO Technical Report No. 13). From previous work (Soifer *et al.* 1980) methane was known to be the dominant absorber for the combined Pluto–Charon system. The two strongest bands for methane in the near-infrared are at 1.7 and 2.35 μm; two additional filters were used to measure the nearby continuum at 1.5 and 2.0 μm. The infrared photometer was set to cycle automatically through these filters; each cycle took approximately fifteen minutes. After every two cycles a set of similar measurements were obtained on SAO 120599, a nearby G0V star expected to have colors identical to those of the Sun. Our observations are summarized in Table 2.1, and depicted graphically as Figure 2.2.

Notice that the flux values (and their associated error bars) are a factor of 2 smaller than those originally published in Marcialis *et al.* (1987), Table 1. This is due to an error in averaging in the original reduction process; the current values tabulated are in fact the correct ones. (Values from the *Science* paper imply an albedo for Pluto much greater than unity, which is how the error was detected).

It should be noticed that the out-of-eclipse lightcurve slope persists during totality. This is in itself proof that the albedo "spots" first proposed by Marcialis (1983, 1988) do in fact reside *on Pluto*, and *not* on the satellite.

2.3. Interpretation

The occultation appears strongly in the two methane bands, indicating that a significant percentage of the light from the combined system comes from Charon. To our surprise, the event was virtually undetected at 2.0 μm. Evidently Charon is much darker than Pluto at this wavelength (which corresponds to methane *continuum*, so subtracting it from the system has negligible effect. If Charon contributed only a smooth continuum to the total light, then the strength of the methane band absorption would be expected to increase as the event reached

Measured Pluto flux densities 1987 March 03

Time of observation (U.T.)	Wavelength (μm)			
	1.5	1.7	2.0	2.35
7.967	14.25 ± 0.15	7.78 ± 0.08	8.15 ± 0.28	2.24 ± 0.11
8.641	14.06 ± 0.15	7.96 ± 0.08	8.30 ± 0.28	2.34 ± 0.11
9.364	12.93 ± 0.17	7.37 ± 0.08	8.13 ± 0.28	2.30 ± 0.11
9.991	12.33 ± 0.13	6.60 ± 0.09	7.72 ± 0.28	1.71 ± 0.12
10.647	12.30 ± 0.13	6.54 ± 0.08	8.32 ± 0.20	1.81 ± 0.11
11.281	12.20 ± 0.17	6.52 ± 0.08	7.99 ± 0.28	1.78 ± 0.11
11.915	12.18 ± 0.17	6.45 ± 0.09	7.57 ± 0.29	1.76 ± 0.11
12.516	12.55 ± 0.13	6.94 ± 0.08	7.91 ± 0.29	2.09 ± 0.11
13.133	13.54 ± 0.13	7.71 ± 0.08	8.04 ± 0.29	2.34 ± 0.11

Table 2.1. Measured flux densities (in mJy) versus time. The calibration of Campins *et al.* (1985) has been assumed. Formal error bars were determined by computing the standard deviation of each datum from the out-of-eclipse lightcurve slope of 0.6 percent hr^{-1}. Thus, they reflect not only uncertainties due to photon statistics and the atmospheric extinction determination, but are a true estimate of the reproducibility of the data as well.

totality; if Charon were as covered with methane as is Pluto, the band strengths would have remained the same throughout the event. Since neither situation held, Charon must be covered with some spectrally active material other than methane.

Comparison data subsets obtained during event, but outside of totality, shows that the leading and trailing crescents of Charon are identical in both albedo and spectral signature, to within the precision of the data.

The spectral differences between Pluto and Charon are best illustrated by using the data in and out of occultation to derive plots of relative reflectance for the two objects, as shown in Figure 2.3. The reflectances have been normalized to unity

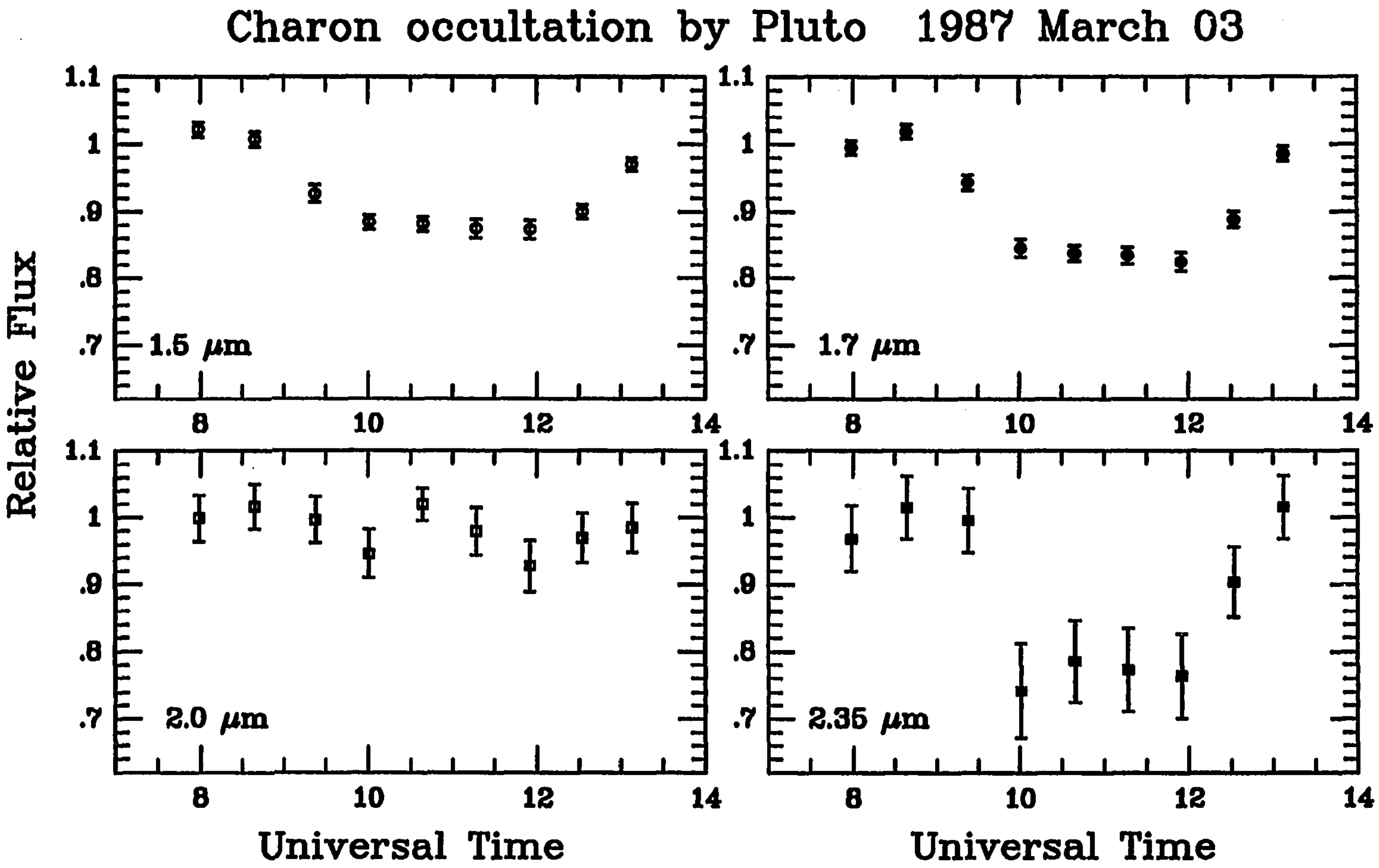

Figure 2.2. Measured fluxes *vs.* time, normalized to their mean values outside of the event. Note that at 2.0 μm the event is virtually undetected. At all wavelengths but 2.35 μm, an out-of-eclipse lightcurve slope of approximately 0.6 percent per hour is visible. Persistence of this slope during totality constitutes proof that the albedo features first proposed by Marcialis (1983, 1984) reside on Pluto, not on Charon.

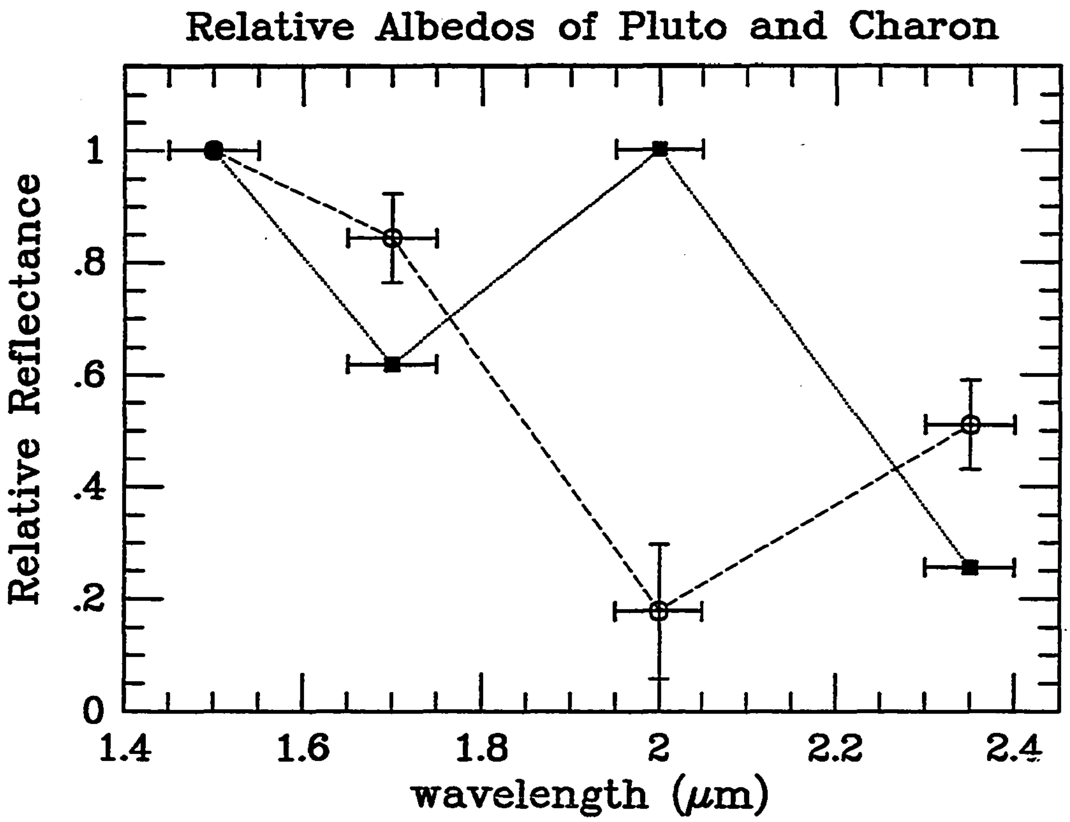

Figure 2.3. Relative albedos for Pluto (▪) and Charon (⊕), normalized to their individual reflectances at 1.5 μm. The small (∼1%) error in the 1.5 micron measures has been propagated to the other three wavelengths. Owing to its much stronger signal, formal errors in Pluto's spectrum are smaller than the plotted symbols.

at 1.5 μm; errors in the 1.5-μm point have been absorbed in the error estimates at the other wavelengths.

Pluto shows the previously known strong methane absorptions at 1.7 and 2.35 μm, first identified by Cruikshank *et al.* (1976) and confirmed by Lebofsky *et al.* (1979). Since that time, the physical state of this methane has been under debate (Cruikshank *et al.* 1977, Fink *et al.* 1980). Buie (Buie and Fink 1987) demonstrated that, at least in the 0.5 to 1.0 μm region, it is not possible to distinguish between the pure frost, pure gas, or the (frost + gas) cases. However, the spectrum of Charon is radically different from that of Pluto.

Several types of ices may be excluded by comparison of our data to laboratory spectra. These include not only CH_4 (see Pluto spectrum for its signature), but also CO_2 (2.0 μm absorption too shallow, no absorption at 2.35 μm); H_2S (2.35 μm absorption too shallow); NH_4SH (2.0 and 2.35-μm depths reversed); and NH_3 (1.5 and 1.7-μm depths reversed, 2.0 and 2.35 μm absorptions too deep).

The most plausible candidate is H_2O ice. Water ice has an extremely strong absorption at 2.0 μm, and another which is moderately strong at 2.4 μm (Fink and Sill 1982). At 55 °K, the 1.5 μm and 1.7-μm reflectances of water ice are similar (Fink and Larson, 1975), although at warmer temperatures the 1.65 μm absorption band is relatively weak. Figure 2.4 shows a spectrum of 55 °K water ice with our data superposed. The agreement with the spectrum of Charon is good, although the 1.5/1.7 μm ratio still differs by about 2 standard deviations from that expected for pure, fine-grained frost.

The water absorption feature at 1.65 μm is known to deepen as grain size is increased (Fink and Larson 1975). Further, our filter at 1.5 μm is located on the steep short-wavelength side of the 1.55-μm absorption. A small shift in the effective wavelength of the filter could result in a rather substantial change in the product of available flux and filter response. Although more detailed spectra may reveal other surface constituents, it is likely from our data that water ice dominates the infrared spectrum of Charon.

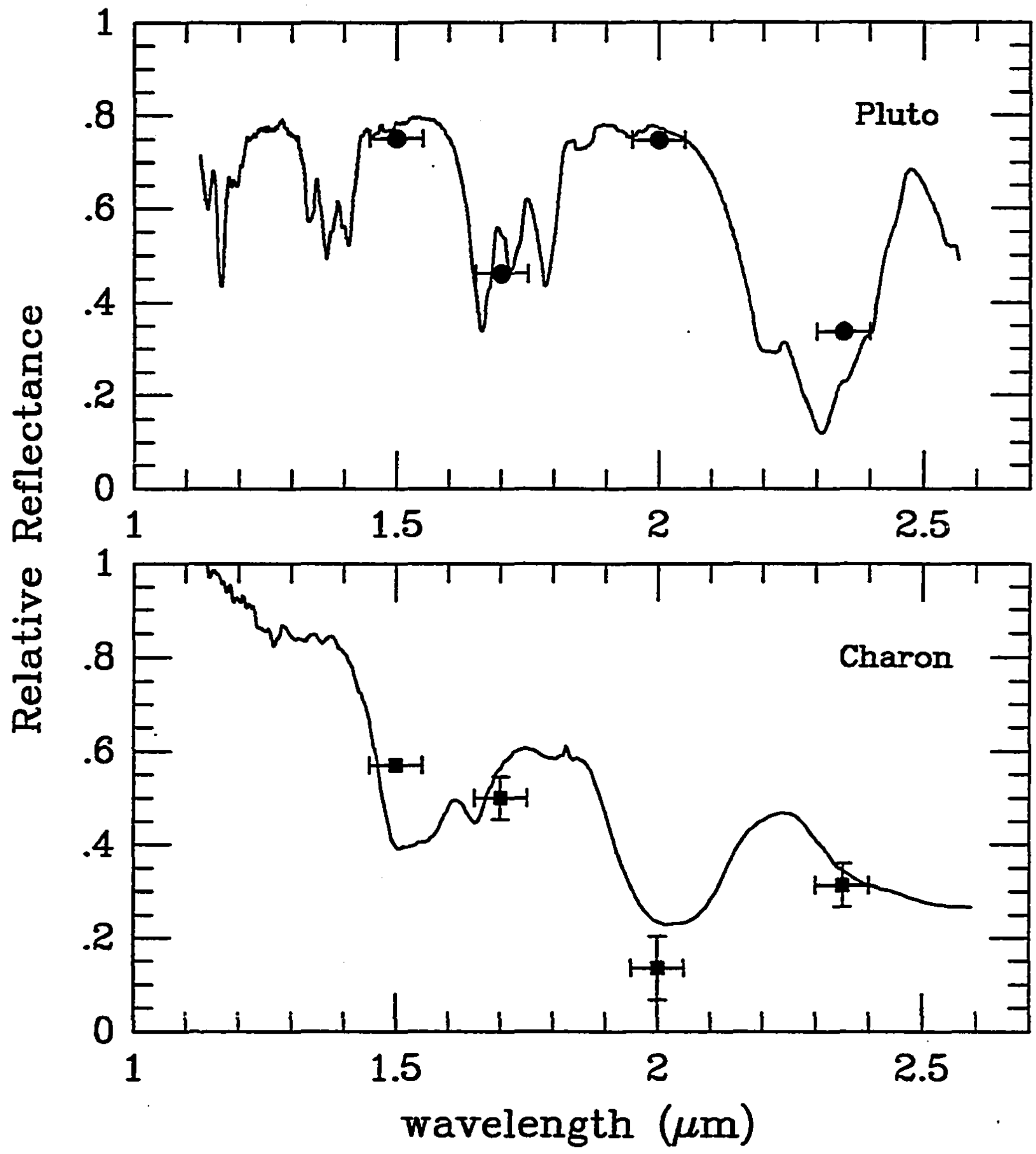

Figure 2.4. Comparison of separate Pluto, Charon spectra to laboratory frosts. (*top*) Pluto's spectrum (•) is typical of methane frost; (*bottom*) Charon's reflectance spectrum (▪) is well-approximated by water ice. Horizontal bars indicate FWHM bandpass for each filter, vertical bars show estimates of overall errors in relative flux determination. Lab data from Fink and Larson (1975).

2.4. Discussion

Presumably, both Pluto and Charon have resided at the same place in the solar system since their formation. Why, then, should such a severe compositional dichotomy exist?

Preliminary analysis of the partial events observed in 1985 and 1986 (Dunbar and Tedesco 1980) shows the visual albedo of Charon to be about half that of Pluto. Thus Pluto is expected to have a lower surface temperature than Charon. Assuming a temperature of 50 °K for Pluto, Charon's temperature would be near 58 °K. The vapor pressure of methane rises exponentially with temperature in this regime, from 3.5 μbar at 50 °K to 59 μbar at 58 °K (Brown and Ziegler 1979). Since the root-mean-square thermal velocity of methane is $\sim 1/2$ escape velocity from Charon to infinity, and an even greater fraction for transfer through the inner Lagrange point onto Pluto, it is easy to show that Charon's inventory of methane would be lost on a timescale short compared to the age of the solar system, whether by Jeans escape or hydrodynamic blowoff. An analysis of volatile escape from Charon appears in the following Chapter.

The details of the partitioning of methane between escape to infinity and transfer onto Pluto are as yet unclear, but escape of up to 27 km of methane from Charon can occur over the age of the solar system. After shedding several kilometers of methane, the surface of Charon would be expected to resemble a global "moraine," with the residuum composed of (cosmically abundant) water ice and a "slag" of darker carbonaceous and/or silicaceous impurities. This process could explain both the compositional difference and also why Charon's visual albedo is significantly less than that of Pluto (Tholen and Buie 1989).

CHAPTER 3

ESCAPE OF METHANE FROM CHARON

3.1. Background

The observations reported in the preceding chapter have demonstrated that while Pluto's spectrum is dominated by methane, Charon shows only a water frost signature. This result was unanticipated prior to the onset of the mutual events. For lack of concrete evidence to the contrary (*Entia non sunt multiplicanda præter necessitatem*, a.k.a. Ockham's, Occam's, or Okkam's razor), Pluto and Charon were expected to have very similar surfaces. Yet the observed dichotomy in surface composition begs explanation from a theoretical standpoint. In this Chapter we address two questions: First, is the observed compositional dichotomy consistent with theory; Second, assuming an initial methane inventory comparable to that of Pluto, where did this methane go. Since it is unlikely that Pluto could have acquired its methane sometime after accretion through some mechanism not equally applicable to Charon, the more logical alternative is that Charon somehow has lost its initial inventory.

Jeans (1925) proposed that thermal escape from the top of an atmosphere could purge a planet of its lighter gases in an extremely efficient manner. Assuming an atmosphere in (local) thermodynamic equilibrium, molecules at the high end of the Boltzmann distribution would be moving at velocities much greater than rms thermal. Define a potential energy variable λ as the ratio of gravitational potential over kT:

$$\lambda = \frac{GMm}{kTr} = \left(\frac{v_{esc}}{U}\right)^2 = \frac{r}{H} \tag{3.1}$$

where G is the universal constant of gravitation, M is the planet's mass, r is the distance from the center, k is Boltzmann's constant, T is temperature, v_{esc} is escape velocity from level r, $U = \sqrt{2kT/m}$, and H is the local scale height.

Jeans showed that for values of λ greater than 2 to 3, a single-component atmosphere (of monatomic gas) could be lost over a timescale of a billion years or less. This theory is unrealistic in several respects. For example, removing the high-energy tail of the Maxwell-Boltzmann distribution causes the gas to re-equilibrate at a temperature lower than its original temperature. Another way of looking at this is that the escaping gas is, in fact, an expanding gas, and gases cool when expanded. In the simple Jeans escape theory, deviations from true LTE are not considered. If the gas is collisionless enough to permit escape to infinity, then it is clearly not collisional enough to justify the assumption of LTE. (That is, *local* no longer has realistic meaning.) Spitzer (1952) showed that significant errors are introduced by neglecting the detailed temperature structure of the atmosphere. Nonthermal mechanisms of escape are also neglected, but at present the details of such are much more speculative.

Over the years, the Jeans theory has been reexamined, modified, made more complex, and otherwise changed by others, such as Õpik, Shklovskiĭ, and Parker. Each modification has lengthened the amount of time predicted for a planet to shed its atmosphere, to the point where $\lambda \sim 1.5$ is required for substantial escape to occur ($\sim$2.5 for a diatomic gas). A good synopsis of the evolution of this theory is given by Hunten (1973) and references therein.

A more modern incarnation of the theory of escape is that of hydrodynamic blowoff (although it too neglects nonthermal escape mechanisms). Hydrodynamic blowoff differs from the above Jeans theory in that it permits, where necessary, a substantial fraction of the thermospheric energy budget to be used to power the escape. For atmospheres as tenuous as those of Pluto and Charon, this is certainly a more realistic approximation. A good summary of how this theory may be applied to the planet of your choice is given in Watson, Donahue, and Walker (1981).

Trafton (1980) applied the theory of Watson *et al.* to Pluto, and came to the conclusion that a methane ball of twice Pluto's mass easily could have evaporated to infinity over the lifetime of the solar system. Therefore, in an effort to save Pluto, he invoked a mystery gas (argon) which was spectrally inactive, but served to impede rapid escape of the methane. However, even argon has a blowoff time constant of ~900 Myr. He therefore was forced to postulate that Pluto's mass was substantially larger than the observations of the day indicated. From mutual event observations, we know this is not so. The only way Trafton could "save" Pluto from itself was to hope that the residuüm of materials left behind (primarily water ice) could insulate methane ice from the vacuum above and "choke off" the outflow, although this explanation is inconsistent with the observed spectral signature of Pluto today. His calculations showed that this would occur when the inert layer reached a thickness of about 87 meters.

Hunten and Watson (1982) showed that the problem could be made to disappear if the energy balance and thermal structure of the atmosphere is considered. As mentioned above, Trafton's assumption of an isothermal atmosphere is not valid in the case of Pluto. Adiabatic expansion (outflow) of a gas causes the gas to cool. Thus, the process of hydrodynamic escape is limited to how fast energy (solar UV) can be injected into the atmosphere, and how rapidly this energy can be conducted away from the deposition level. Hunten and Watson showed that the level of energy implantation was at about 3.5 $R_{\rm P}$. Below this level, gas expansion causes a deep temperature minimum. By fixing the temperature minimum to be absolute zero, an upper limit on the methane escape flux is calculable. Pluto need shed only about 3 km of methane over the lifetime of the solar system. The presence of dense atmospheric constituents such as argon or carbon monoxide, should they exist, will limit further the amount of methane lost.

It is precisely the theory presented in Watson *et al.* (1981) and reiterated in Hunten and Watson (1982) that we apply to Charon. Similar calculations were performed concurrently, but independently, by Trafton *et al.* (1988).

3.2. Calculation

For Charon, we assume the radius in Tholen and Buie (1989), and assume that its density is similar to the mean of the Pluto–Charon system, namely 2.030 gm cm^{-3}. Other assumed and derived quantities are given in Table 3.1. We use these values to solve simultaneously the nonlinear system of equations (1) and (2) from Hunten and Watson:

$$\left.\begin{aligned} \zeta_{max} &= \frac{1}{S}\left[\frac{(\lambda_1/2)^S+1}{\lambda_o-\lambda_1}\right]^2 \\ \lambda_1^2 &= \frac{\beta}{\lambda_o\zeta_{max}-(\zeta_{max}/S)^{1/2}} \end{aligned}\right\} . \tag{3.2}$$

For convenience of calculation, the nondimensional variables

$$\zeta = F \cdot \left(k^2 T_o / \kappa_o GMm\right) \tag{3.3}$$

and

$$\beta = \dot{E} \cdot \left(GMm / kT_o^2 \kappa_o\right) \tag{3.4}$$

are introduced. ζ and β are the flux of escaping particles and the EUV heating rate, respectively. F and $\dot{E}$ correspond to these quantities when evaluated in cgs units. The thermal conductivity of methane is $\kappa = \kappa_o (T/T_o)^s$, and $S = (s+1)/2 = 1.06$ in the preceding equations.

Assumed and derived quantities for Charon

Quantity	Symbol	Value	Units
⟨Geometric Albedo⟩	p	0.377	
Johnson Blue magnitude	B	$+16^{m}\!.76$	
Charon radius	r_o	593	km
Charon density	ρ	2.030	gm cm^{-3}
Charon mass	M	1.773×10^{24}	gm
Surface gravity	GM/r_o^2	33.63	cm sec^{-2}
Surface Temperature	T_o	55	°K
CH_4 conductivity at T_o	κ_o	450	erg cm^{-1} $°K^{-1} sec^{-1}$
Power of T	s	1.12	
Escape parameter	$\lambda_o = GMm/kT_o r_o$	6.979	
Unit of solar flux	$\kappa_o T_o / \lambda_o r_o$	5.98×10^{-5}	erg $cm^{-2} sec^{-1}$
Unit of escape flux at r_o	$\kappa \lambda_o / k r_o$	3.84×10^{11}	$cm^{-2} sec^{-1}$
Methane molecular mass	m	2.657×10^{-23}	gm

Table 3.1. Parameters used for calculation of methane escape flux from Charon. Dimensions specific to Charon are adopted from Tholen and Buie (1989); thermal parameters from Hunten and Watson (1982).

3.3. Results

The coupled system (3.2) can be solved for ζ_{max} and λ_1 with the aid of a hand calculator and a couple of beers. A graphical solution is presented as Figure 3.1. Results are summarized in Table 3.2 below.

According to the models of Lupo and Lewis (1980*a*, *b*), and more recently those of Simonelli *et al.* (1989), Simonelli and Reynolds (1989), and McKinnon and Mueller (1988), Charon's total starting inventory of CH_4 was much less than 10 km. Therefore, we conclude that Charon should be expected to be devoid of methane today, which is keeping with the observations.

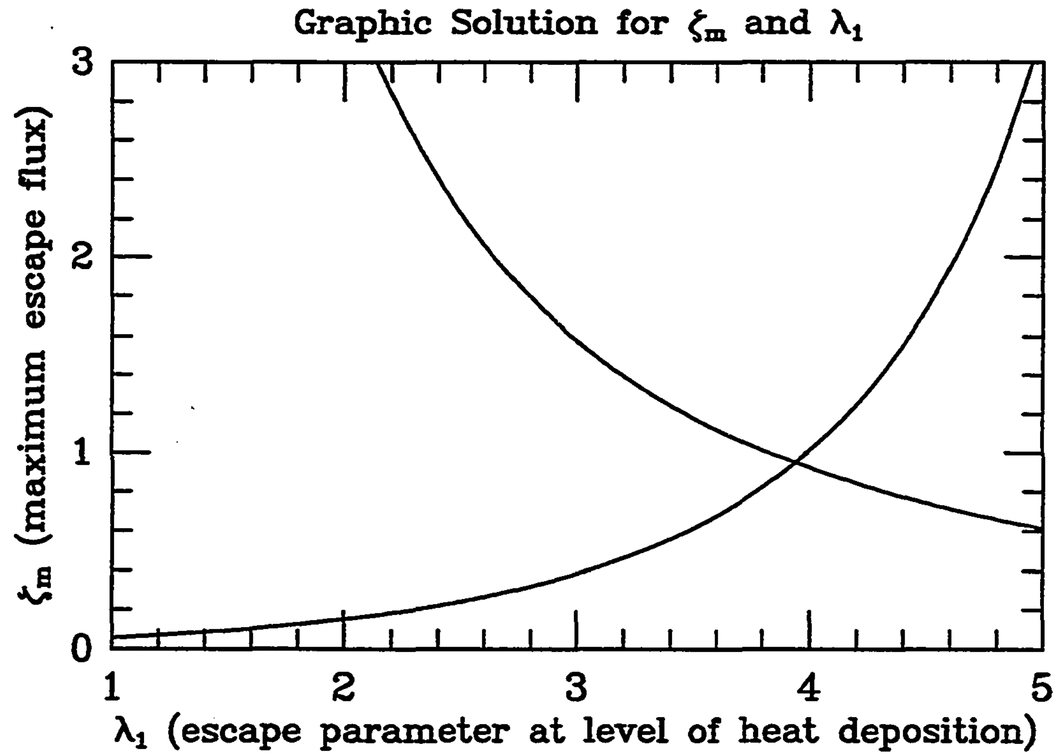

Figure 3.1. Graphical solution of Equation (3.2) verifies the numerical result of $(\lambda_1, \zeta_{max}) = (3.9375,\ 0.9489)$ for escape of methane from Charon.

Summary of Results

Quantity	Value	Units
Solar flux	5×10^{-4}	erg $cm^{-2}sec^{-1}$
β Energy parameter	88	
λ_1 Escape level parameter	3.937	
ζ_{max} Escape flux parameter	0.949	
Escape flux at r_o	3.66×10^{11}	$cm^{-2}sec^{-1}$
Energy implantation level	1.77	R_{Ch}
Ice lost in:		
1 sec	1.91×10^{-11}	cm
1 Pluto year	1.5	mm
4.5 Gyr	27.1	km

Table 3.2. Derived methane escape rate from Charon. Note the results are in very favorable agreement with the 31 km Gyr^{-1} result of Trafton *et al.* (1988).

It is important to note that using the treatment of Hunten and Watson, we have calculated only an *upper limit* to the amount of methane which could have been blown off. However, note also that we have assumed the solar UV flux shortward of 1000 Å has always been what is today, and a heating efficiency of 50 percent. Presumably, the Sun went through a period of enhanced ultraviolet flux early in its history (*cf.* Hunten *et al.* 1989, and references cited there). We have further assumed that the Pluto–Charon system has resided at 39.5 AU for the entire lifetime of the solar system. Finally, we have neglected nonthermal sources of energy, such as impact bombardment by soft electrons. This latter source was considered by Hunten and Watson, who claim that up to 20 times the energy implantation rates we have adopted might have been available.

As noted by Hubbard (personal communication), one further piece of observational evidence deserves mention. A stellar occultation by Charon was observed by Walker (1980). The shape of the occultation light curve (2 sec time resolution) shows no deviation from a perfectly symmetric square-well shape. Transitions between totality and out-of-event values are abrupt, last $\leq$4 sec, and show no sign of refraction by a thin atmosphere. From this event, it may be concluded that presently Charon has no atmosphere with surface pressure greater than a few microbars (the vapor pressure over the solid at 55 °K), or thicker than ~96 km.

3.4. Where did the methane go?

If Charon were sitting alone in its orbit, the obvious answer to this question is that the CH_4 all escaped to infinity. However, the presence of Pluto clearly is a large perturbation on the system. With a few simplifying assumptions, it is possible to make a rough estimate as to how the presence of Pluto alters the problem.

Charon's inner Lagrange point lies at a distance of 3.99 R_{Ch}. If the escape level r_1 is at 1.77 R_{Ch}, then

$$\frac{\Delta GPE\,(r_1 \rightarrow r_{L_1})}{\Delta GPE\,(r_1 \rightarrow \infty\,)} = 0.556\,. \tag{3.5}$$

That is, flow from the escape level to the inner Lagrange point requires only about 1/2 the energy needed to escape from an isolated Charon. Clearly, there is an angularly-dependent attenuation term which arises from the ejection geometry. Nonetheless, from the standpoint of energetics, this crude, back of the envelope calculation shows that something on the order of ~1–10% is a realistic *minimum value* for a mass transfer partitioning coefficient. A more quantitative analysis of mass transfer from secondary to primary, from primary back to secondary, and total escape from the binary currently is in progress (Whipple *et al.* 1989). The reader is referred to their forthcoming paper for further details.

As a final comment, note that if Pluto's surface is predominantly methane, and Charon's predominantly water ice, then the rheologies at 50–55 °K are likely to differ significantly (Marcialis, 1985; 1989*a,b*). Due to its (comparatively) larger gravity and *much* less viscous working material, Pluto's surface probably bears the scars of a much more contemporary impactor population than does Charon. If we can assume that both bodies have been in association since the end of the heavy bombardment era, then images of their surfaces may tell us much about the flux of impactors *vs.* time. Yet another parallel between the Earth–Moon and Pluto–Charon systems may emerge.

CHAPTER 4

CVF SPECTROPHOTOMETRY OF PLUTO: CORRELATION OF COMPOSITION WITH ALBEDO

Time-resolved spectrophotometry of the Pluto–Charon system was obtained on 6 nights in March and April of 1988. The observations include about 1/3 of the 6.4-day light curve, centered around minimum light, and span the wavelength region from 0.96 to 2.65 μm. The spectra reveal night-to-night variations in depths of methane absorptions throughout this region. Band depths vary such that their equivalent width is least near minimum light. One obvious interpretation is that dark regions on the planet are depleted in methane relative to bright areas, at least for the hemisphere observed. Our results are consistent with the observations of Buie and Fink (1987) but in conflict with those of Sawyer (1989). The near-infrared spectrum of Pluto appears to be dominated by surface frost; atmospheric methane contributes much less to the overall spectral signature. We see evidence that Pluto's dark equatorial regions tend to be redder than those of more moderate albedo.

4.1. Introduction

Infrared photometry of Pluto by Cruikshank *et al.* (1976) and Lebofsky *et al.* (1979), along with visual/near-infrared spectroscopy by several groups (*e.g.*, Fink *et al.* 1980; Soifer *et al.* 1980) have demonstrated conclusively the existence of methane in the combined light of the Pluto–Charon system. The mutual events allowed Marcialis *et al.* (1987) to determine that the spectral signature of methane could be attributed wholly to Pluto; Charon's surface is consistent with that of water frost.

CCD spectrophotometry of the Pluto–Charon system in 1983 (Buie 1984; Buie and Fink 1987) shows methane absorption features that seem to vary with rotational phase. However, similar observations spanning many nights in the period 1983–1989 (Sawyer 1986, 1989; Sawyer *et al.* 1987) apparently are in conflict with the results of Buie and Fink.

To resolve these discrepant results regarding rotational variability of Pluto's methane, and to test whether albedo and composition are correlated, we undertook a program to observe Pluto during the 1988 apparition.

4.2. Observations

To increase the sensitivity of our observations, Pluto was observed in the 1.0- to 2.6-μm region of the spectrum. As for most other cosmically abundant frosts, the spectral activity of methane is much greater at near-infrared wavelengths than in the visual region of the spectrum.

Observations reported here were made with the liquid He-cooled InSb infrared photometers RC1 and PRIMO at NASA's 3-m Infrared Telescope Facility (IRTF) on Mauna Kea, Hawaii. Dates, times, and detectors used for the observations are reported in Table 4.1. The University of Hawaii double CVF (circularly-variable filter) was used to step through 22 different wavelengths in the spectral region from 1 μm to 2.65 μm. This CVF has spectral resolutions ($\Delta\lambda/\lambda$) of 3% and 5% in the short- and long-wavelength halves, respectively. The switch from short half to long half was made at about 1.5 μm, with one channel of overlap to ensure that both halves had a common zero point. The telluric water absorption at 1.40 μm, along with the "CVFCAL" program written by M. Buie, were used to calibrate the wavelength scale.

Log of IRTF Pluto observations, 1988

Date	UT Times	No. Scans	r (AU)	Δ (AU)	α (deg)	θ_{rot}	Dewar	Comments
March 08	1540 – 1620	1	29.669	29.098	–1.59	0.85	RC1	cloudy < 1300
March 09	1130 – 1500	3	29.669	29.086	–1.57	0.00	RC1	
March 10	1110 – 1350	3	29.669	29.073	–1.55	0.15	RC1	occ. cirrus
March 11		0					RC1	winded out
April 15	0845 – 1320	4	29.668	28.740	–0.75	0.78	PRIMO	
April 16	1230 – 1330	1	29.668	28.735	–0.73	0.94	PRIMO	cloudy < 1200
April 17	0820 – 1130	3	29.668	28.732	–0.71	0.08	PRIMO	superb night

Table 4.1. Listed are times and circumstances of the observations. r, Δ, α, and θ_{rot} are heliocentric and geocentric distance, solar phase angle, and rotational phase, respectively.

Each scan of Pluto's spectrum required 40–45 minutes to complete. At each wavelength step, one measurement of Pluto was taken as the mean of 10 separate 4-second integrations. Measurements were made through a 4-mm aperture (7″.8 in the sky plane), relative to sky reference areas 20″ north and south of the object.

The nearby star SAO 120107 (= HD 120050) was used as the primary comparison object. This solar-type star has been used as a flux standard at many wavelengths for study of Pluto throughout the mutual event season, and defines the zero point (at least at visual wavelengths) to which the "Johnson Pluto system" is referenced (*cf.* Tholen *et al.* 1987*b*). SAO 120107 typically was observed both before and after each scan of Pluto. As a check on the nightly extinction coefficient determinations, we also observed the solar analog 16 Cyg B. Reproducibility was found to be excellent.

Figure 4.1 depicts the mean rotational phase of Pluto on those six nights where data were obtained.

4.3. Results

In order to present the data in a reasonably compact form, we tabulate only the mean UT for each scan, uncorrected for light-travel time, in Tables 4.2–4.5. Ordinates are differential magnitudes in the usual sense (Pluto–SAO 120107), but have been reduced to mean distance on the night of April 17 using values of r and Δ in Table 4.1. No solar phase coefficient β has been applied to the data.

The March and April observations are plotted in Figures 4.2 and 4.3, respectively, with nightly mean rotational phase indicated on each panel.

It must be remembered that the combined light curve of Pluto–Charon changes systematically in intensity by as much as several (3–10) millimag hr^{-1} (see Figure 4.1). Particularly for those nights when the PRIMO detector was used and the light curve was not at an extremum, this variation is apparent from scan to scan within the night. That such systematic variations are seen in the data is evidence the calculated error bars are reasonable ones. Such variations should be taken into account when using the data for detailed lightcurve analysis.

For those nights where multiple spectra of Pluto were obtained, it is barely possible to calculate mean lightcurve slopes at each wavelength, and thus to reduce each spectrum to a common epoch. These small (<1%) corrections have no significant bearing upon the present analysis, and *have not* been applied to the data.

If the plots are laid out on facing pages, rotational phase increases in the normal reading sense (left to right, top to bottom). Due to the large dynamic range

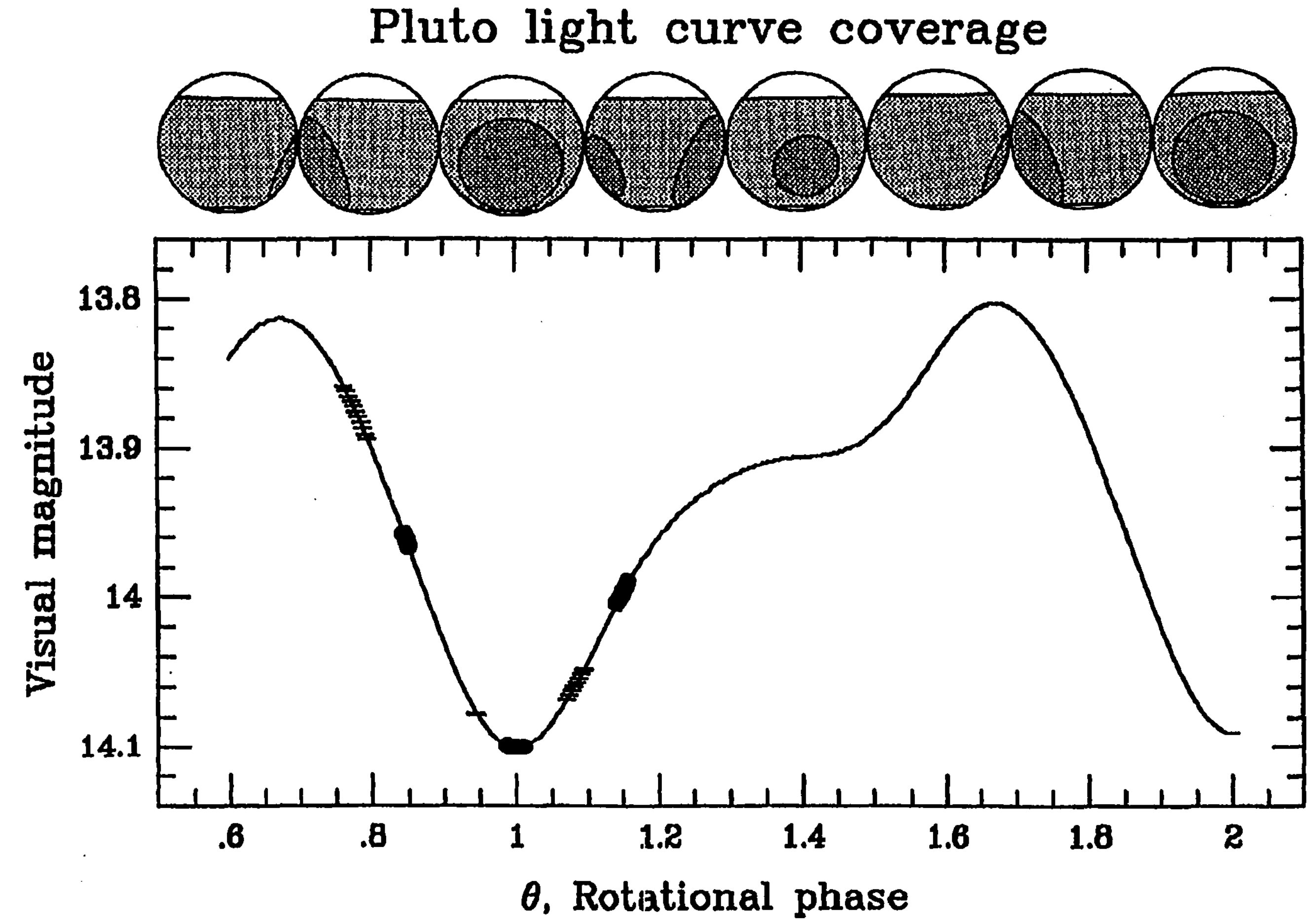

Figure 4.1. Portions of light curve sampled on the six nights data were obtained. Solid regions: 1988 March 08, 09, 10; hatched regions: 1988 April 15, 16, 17. Corresponding images of the two spot model are included for reference.

Summary of observations, 1988 March 08–09

$\lambda(\mu m)$	Δm (mag)	σ	Δm (mag)	σ	Δm (mag)	σ	Δm (mag)	σ
0.963	4.531	0.019	4.509	0.021	4.489	0.017	4.576	0.008
1.034	4.491	0.034	4.543	0.060	4.526	0.029	4.592	0.014
1.105	4.489	0.027	4.492	0.015	4.566	0.040	4.576	0.011
1.176	4.710	0.045	4.785	0.033	4.760	0.030	4.793	0.017
1.248	4.419	0.037	4.469	0.028	4.523	0.011	4.504	0.026
1.319	4.546	0.045	4.679	0.039	4.739	0.015	4.621	0.036
1.392	4.814	0.106	5.025	0.145	5.017	0.156	5.000	0.033
1.428	4.610	0.030	4.616	0.042	4.561	0.055	4.685	0.233
1.464	—	—	4.632	0.029	4.690	0.043	4.617	0.031
1.537	—	—	4.646	0.047	4.686	0.037	4.710	0.019
1.540	4.612	0.018	4.664	0.014	4.681	0.012	4.672	0.022
1.649	4.991	0.017	4.991	0.026	4.982	0.012	4.964	0.021
1.756	4.854	0.028	4.925	0.025	4.920	0.005	4.888	0.010
1.862	4.620	0.022	4.779	0.030	4.769	0.020	4.783	0.040
1.966	4.683	0.012	4.766	0.014	4.762	0.010	4.782	0.016
2.069	4.836	0.011	4.894	0.023	4.893	0.009	4.898	0.020
2.169	5.151	0.019	5.117	0.022	5.142	0.015	5.111	0.021
2.268	5.425	0.029	5.393	0.025	5.448	0.016	5.430	0.024
2.365	5.487	0.044	5.537	0.025	5.487	0.023	5.551	0.031
2.460	5.208	0.043	5.239	0.078	5.205	0.043	5.287	0.062
2.554	4.813	0.097	4.504	0.191	4.864	0.108	4.705	0.089
2.646	4.153	0.555	3.782	0.479	3.569	0.675	4.571	0.948
Date:	March 08		March 09		March 09		March 09	
⟨UT⟩:	15.96		11.97		13.16		14.13	
corr:	$-0\overset{m}{.}0276$		$-0\overset{m}{.}0267$		$-0\overset{m}{.}0267$		$-0\overset{m}{.}0267$	

Table 4.2. Tabulated are spectra obtained on 1988 March 08 and 09. Date and mean geocentric UT of each scan appear at the bottom. Also tabulated are the distance corrections applied (in magnitudes) in order to bring all data to the geometry of the 1988 April 17 observations.

Summary of observations, 1988 March 10

$\lambda(\mu m)$	Δm (mag)	σ	Δm (mag)	σ	Δm (mag)	σ
0.963	4.565	0.045	4.403	0.017	4.540	0.036
1.034	4.802	0.042	4.512	0.023	4.544	0.010
1.105	4.622	0.035	4.454	0.027	4.521	0.023
1.176	5.005	0.046	4.733	0.034	4.862	0.060
1.248	4.552	0.023	4.413	0.013	4.557	0.045
1.319	4.518	0.019	4.570	0.009	4.724	0.043
1.392	4.672	0.078	4.751	0.182	4.842	0.121
1.428	4.550	0.153	4.560	0.071	4.694	0.032
1.464	4.561	0.037	4.699	0.059	4.641	0.081
1.537	4.539	0.024	4.540	0.020	4.642	0.049
1.540	4.570	0.019	4.596	0.016	4.669	0.027
1.649	5.009	0.019	4.996	0.029	5.050	0.032
1.756	4.893	0.019	4.935	0.022	4.967	0.047
1.862	4.660	0.015	4.770	0.048	4.629	0.036
1.966	4.441	0.017	4.583	0.024	4.750	0.026
2.069	4.956	0.017	4.883	0.022	4.937	0.008
2.169	5.269	0.031	5.228	0.016	5.285	0.043
2.268	5.577	0.034	5.439	0.055	5.519	0.029
2.365	5.740	0.042	5.602	0.025	5.575	0.047
2.460	5.483	0.080	5.326	0.024	5.340	0.031
2.554	5.996	0.133	5.127	0.057	5.249	0.138
2.646	3.433	0.411	5.572	0.915	3.995	0.419
Date:	March 10		March 10		March 10	
$\langle$UT$\rangle$:	11.50		12.67		13.42	
corr:	$-0^{m}.0257$		$-0^{m}.0257$		$-0^{m}.0257$	

Table 4.3. As for the previous Table, but for the 1988 March 10 observations.

Summary of observations, 1988 April 15

λ(μm)	Δm (mag)	σ	Δm (mag)	σ	Δm (mag)	σ	Δm (mag)	σ
0.968	4.342	0.008	4.389	0.007	4.376	0.007	4.387	0.007
1.038	4.375	0.008	4.438	0.010	4.410	0.006	4.411	0.009
1.109	4.357	0.011	4.374	0.010	4.381	0.008	4.393	0.008
1.181	4.642	0.015	4.679	0.015	4.634	0.013	4.661	0.013
1.252	4.334	0.009	4.349	0.009	4.347	0.013	4.350	0.013
1.324	4.512	0.011	4.512	0.015	4.505	0.013	4.482	0.007
1.396	4.840	0.031	4.775	0.042	4.787	0.037	4.804	0.024
1.436	4.448	0.038	4.484	0.065	4.472	0.045	4.601	0.050
1.469	4.555	0.015	4.506	0.010	4.500	0.013	4.506	0.012
1.541	4.499	0.019	4.446	0.008	4.433	0.012	4.463	0.010
1.547	4.504	0.006	4.527	0.008	4.525	0.009	4.494	0.009
1.657	4.897	0.012	4.923	0.009	4.908	0.012	4.909	0.006
1.764	4.853	0.014	4.833	0.009	4.822	0.006	4.821	0.007
1.870	4.569	0.008	4.575	0.012	4.568	0.008	4.575	0.010
1.974	4.569	0.009	4.567	0.008	4.571	0.010	4.574	0.008
2.076	4.724	0.012	4.748	0.011	4.723	0.009	4.728	0.011
2.176	5.075	0.012	5.131	0.011	5.094	0.008	5.089	0.012
2.275	5.410	0.015	5.407	0.018	5.414	0.024	5.403	0.016
2.372	5.571	0.029	5.596	0.033	5.600	0.015	5.538	0.029
2.467	5.068	0.035	5.110	0.032	5.101	0.047	5.105	0.032
2.560	4.649	0.119	4.922	0.094	4.963	0.090	5.113	0.354
2.652	4.574	0.695	4.665	0.742	4.708	0.347	—	—
Date:	April 15		April 15		April 15		April 15	
(UT):	9.15		10.32		11.67		12.92	
corr:	$-0^m_.0006$		$-0^m_.0006$		$-0^m_.0006$		$-0^m_.0006$	

Table 4.4. As for the previous Table, but for the 1988 April 15 observations.

Summary of observations, 1988 April 16–17

$\lambda(\mu m)$	Δm (mag)	σ	Δm (mag)	σ	Δm (mag)	σ	Δm (mag)	σ
0.968	4.559	0.010	4.517	0.007	4.505	0.018	4.476	0.010
1.038	4.547	0.011	4.564	0.009	4.534	0.009	4.528	0.009
1.109	4.525	0.014	4.511	0.008	4.501	0.013	4.483	0.010
1.181	4.731	0.017	4.791	0.013	4.743	0.015	4.737	0.015
1.252	4.464	0.012	4.479	0.012	4.467	0.013	4.431	0.009
1.324	4.598	0.012	4.599	0.013	4.599	0.016	4.624	0.014
1.396	4.751	0.047	4.841	0.020	4.814	0.072	4.789	0.025
1.436	4.640	0.070	4.517	0.040	4.650	0.050	4.577	0.041
1.469	4.634	0.026	4.653	0.017	4.592	0.024	4.577	0.014
1.541	4.607	0.022	4.569	0.012	4.564	0.013	4.456	0.010
1.547	4.639	0.011	4.656	0.014	4.637	0.013	4.630	0.009
1.657	4.913	0.011	4.980	0.014	4.969	0.163	4.976	0.012
1.764	4.835	0.010	4.895	0.013	4.880	0.014	4.874	0.010
1.870	4.545	0.013	4.718	0.011	4.661	0.036	4.656	0.018
1.974	4.737	0.017	4.742	0.009	4.701	0.023	4.677	0.014
2.076	4.852	0.008	4.881	0.011	4.847	0.010	4.833	0.010
2.176	5.079	0.018	5.114	0.018	5.121	0.012	5.134	0.014
2.275	5.297	0.028	5.360	0.015	5.375	0.020	5.386	0.021
2.372	5.410	0.023	5.425	0.024	5.509	0.020	5.522	0.042
2.467	5.175	0.054	5.203	0.045	5.231	0.042	5.200	0.041
2.560	5.025	0.170	5.160	0.114	5.122	0.172	5.111	0.139
2.652	4.078	0.694	—	—	4.907	0.611	4.483	0.479
Date:	April 16		April 17		April 17		April 17	
⟨UT⟩:	13.03		8.71		9.86		10.96	
corr:	$-0\overset{m}{.}0002$		$-0\overset{m}{.}0000$		$-0\overset{m}{.}0000$		$-0\overset{m}{.}0000$	

Table 4.5. As for the previous Table, but for the 1988 April 16 and 17 observations.

inherent in the spectra (~2.5 mag), it is only barely possible to discern night-to-night spectral variations. However, careful study of the absorptions at 1.6–1.8 μm and 2.0–2.5 μm in particular shows that the depths and/or shapes do in fact vary systematically. It happens that at the core of the 1.7 μm absorption there is only a very small light curve during about one day to either side of visual light curve minimum. The increase in continuum level is almost totally negated by a simultaneous increase in absorption depth.

One convenient technique for depicting the variable nature of the absorptions is to take flux ratios of the various nightly mean spectra. Were there no inherent variation, then all absorptions might be expected to divide out to within a constant. This constant is due to the nightly variation in mean brightness. Conversely, if the band depths vary, then a systematic deviation from a constant value would be encountered as an absorption is traversed.

We present two different normalizations to demonstrate different effects. Figure 4.4 depicts the March ratios. Although the spectra do vary over the three nights, there is remarkable symmetry in shape around minimum light. Within a zeropoint correction of about 0.02 mag, deviations from the normalization track each other rather well.

The April ratios (Figure 4.5) use the 0.94 rotational phase data as divisor. Variation is very apparent between rotational phases 0.78 and those close to the lightcurve minimum. As expected from the previous Figure, the differences between phases 0.94 and 0.08 are once again much less pronounced. The deviation at any one wavelength is barely significant when considering the zeropoint correction, but we feel the *systematic* variation enforces the claim that differences are real.

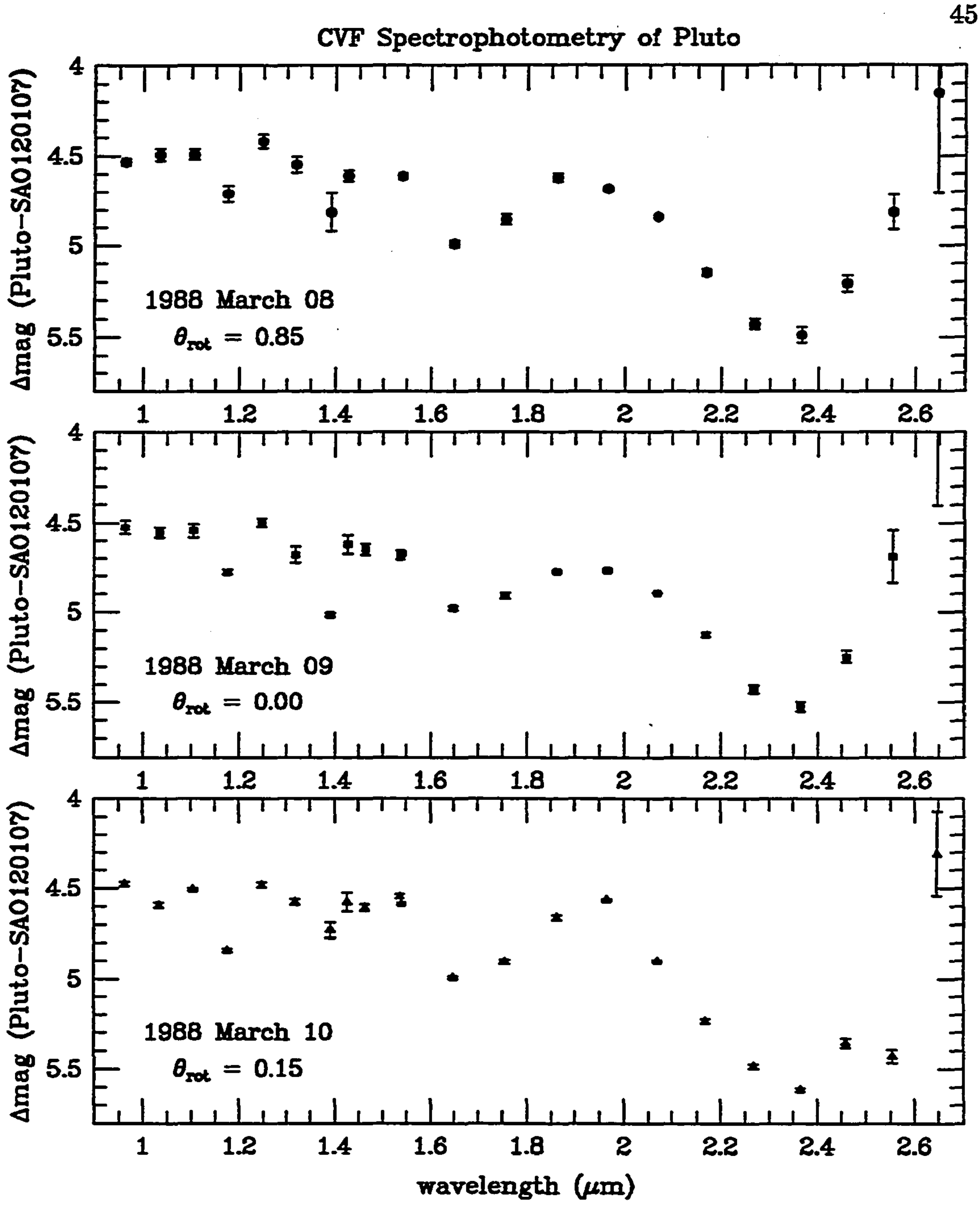

Figure 4.2. Nightly mean Pluto spectra for 1988 March 08, 09 and 10. All absorptions are due to methane. Formal error bars include any variation between scans due to Pluto's light curve.

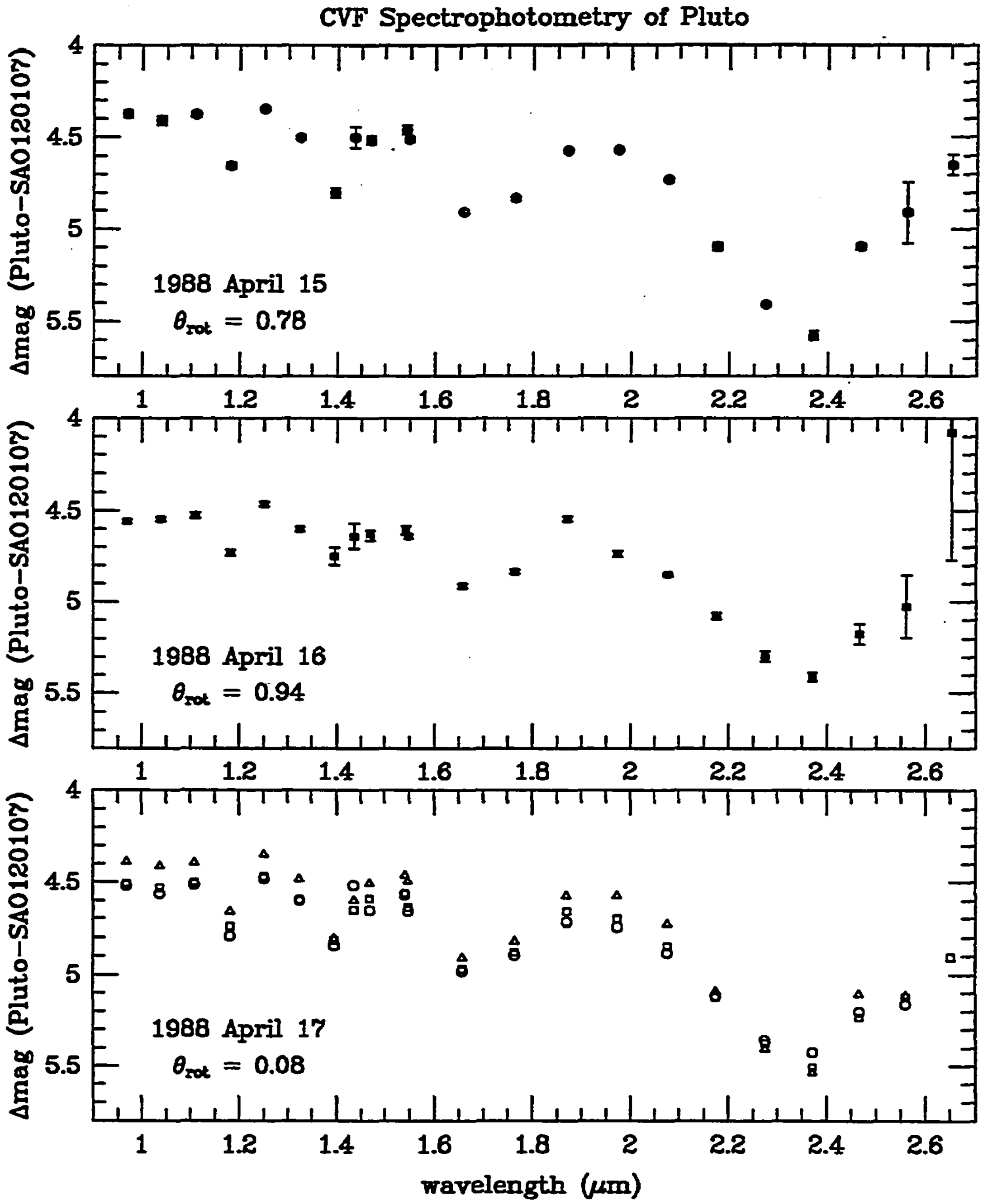

Figure 4.3. Same as the preceding figure, for Pluto spectra obtained 1988 April 15, 16 and 17. In lieu of error bars, individual scans are plotted for April 17. Approximately 70 min elapsed between scans. Systematic scan-to-scan variation is apparent on April 17 and is due to the rotational light curve of Pluto. Note the "negative" light curve in the core of the 2.35 μm band.

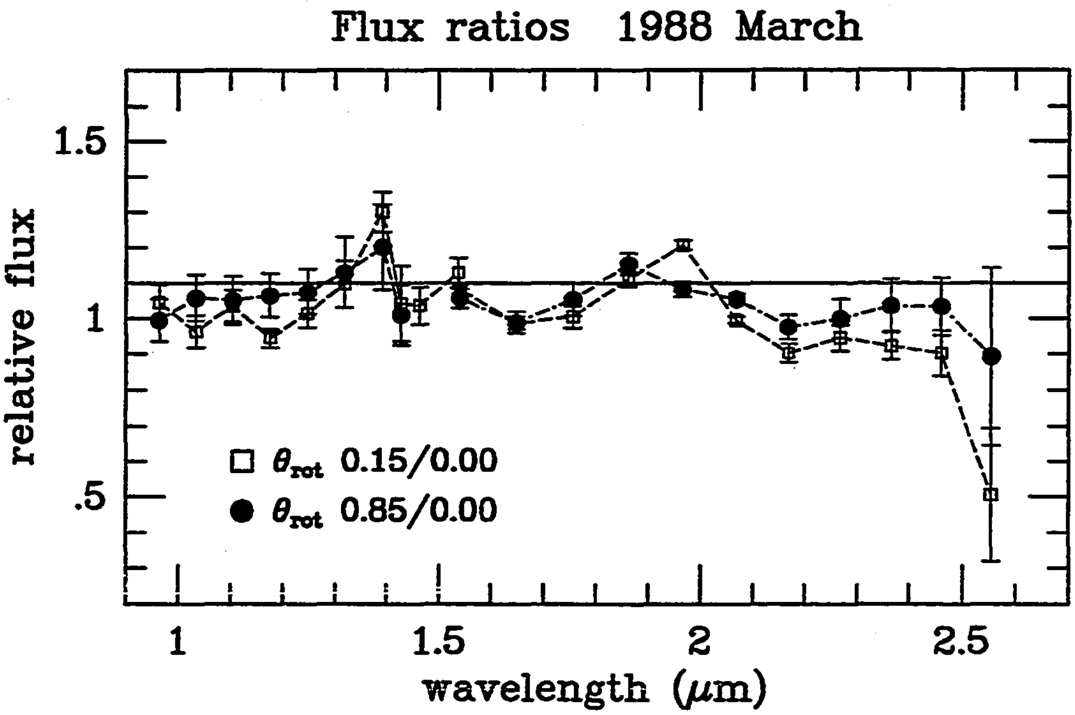

Figure 4.4. Flux ratios for March 08/09 and 10/09 show systematic deviation from a straight line. Probable errors from the divisor have been propagated to the other nightly means, and therefore represent true deviation from a flat line. For clarity, the horizontal line has been shifted upward by 10%, which corresponds approximately to the change in continuum light curve between the three nights. Deviation from a constant ratio is only marginally significant at any one datum, however these deviations are *systematic* across the 1.7- and 2.35-μm absorptions of methane. The ratios are much more similar to each other than to the normalization, demonstrating symmetry about lightcurve minimum.

4.4. Discussion

Marcialis (1983, 1988*a*) constructed an albedo model for the surface of Pluto to explain the rotational and orbital light curve. This model invoked two static dark regions near Pluto's equator to modulate the 6.4-day rotational variation, and two bright, longitudinally-symmetric polar caps as one means of explaining the observed dimming of Pluto over the last 3 decades. A reanalysis by Buie and

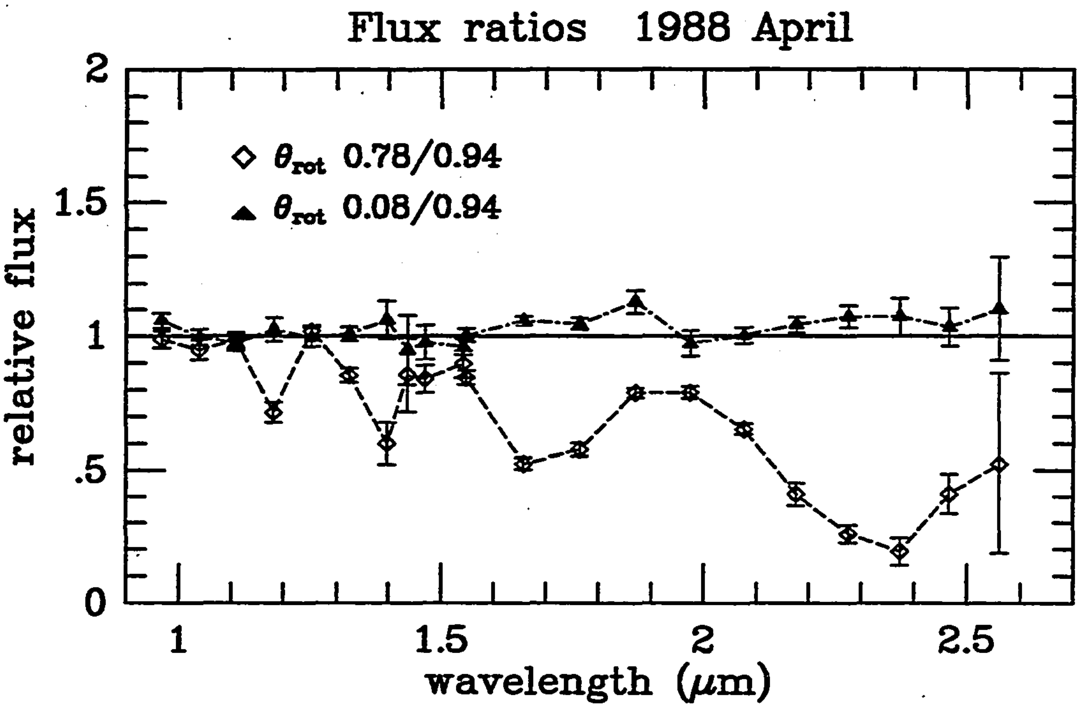

Figure 4.5. As for the previous Figure, but for the April observations. For clarity, the April 15/16 ratio has been shifted downward by 20%, which corresponds to the approximate change in continuum light curve between the two nights. Systematic differences in the April 15 observations demonstrate an unquestionable variation in depth of methane absorptions with rotational phase. A slightly bluish slope in this ratio is evidence that Pluto may be redder at minimum light.

Tholen (1989) gave basically the same results, with the only significant exception being that the smaller equatorial spot might be *bright* and, if so, was positioned in longitude *ahead* of the major dark region (Marcialis 1988*b*). At the observed rotational phases near minimum light, the two models are virtually identical.

The original albedo model was formulated only to explain the light curve of Pluto, and no *a priori* connection was implied between albedo and composition. However, if such a connection were to be assumed, there are two simple possibilities.

That is, dark regions could be either enriched or depleted in methane relative to bright.

If bright regions are rich in methane relative to dark, then one would expect to see the planet's light curve in the band center to be *inversely correlated* with the continuum (visual) light curve. Conversely, if dark regions are rich in methane relative to bright, one would expect both continuum and band center light curves to vary in step with one another, particularly because when the dark regions face earth, less continuum due to the bright areas can dilute the absorptions.

A third possibility is that neither region is particularly enriched in methane with respect to the other. ***Ab initio***, one would expect there to be no variation in absorption with rotational phase. As was first pointed out by Buie (1984), this is not the case. Any albedo distribution not longitudinally symmetric which underlies an optically thin atmosphere tends to modulate the "airmass factor" as the planet rotates. (Airmass factor, η_{eff}, may be defined as the one-way, globally-averaged optical path length, expressed in units of the normal optical path length η_o). For example, if a dark area comprising a substantial portion of a hemisphere were positioned at the sub-Earth point of a fully illuminated planet, then the long slant paths near the limb comprise the dominant contribution to the airmass factor, and η_{eff} would be maximized.

Note that the consequences of these three possibilities are completely general, and therefore immune to the specifics of the albedo model assumed in all but the most pathological or contrived cases.

For completeness, we mention a fourth possibility: the planet could be shrouded by a deep, optically thick atmosphere. In this case, one would expect little variation in the spectrum with rotational phase. However, this case is not acceptable for Pluto as it causes difficulty in explaining the observed 30% brightness fluctuations seen each $6^{d}\!.4$. A transparent upper atmosphere with an optically thick basal haze layer causes similar problems, and therefore such layers with normal optical depth $\tau_o \gtrsim 0.5$ also may be excluded, independent of theoretical considerations (Stansberry *et al.* 1989).

Based upon the results of our observations, the only scenario which gives a consistent explanation is the first one. The near-infrared spectrum is dominated by surface frost, not atmosphere. Albedo and composition (or at least spectral activity of the methane) do indeed seem to be correlated on the surface of Pluto. Bright regions show a more pronounced methane signature in a real and systematic manner. The deep bands at 1.7 and 2.35 μm dominate the substantial modulation of the continuum level. While the much narrower and shallower bands at 1.15 and 1.35 μm are unable to overcome the continuum, they too show some evidence for a variation in their depth, although much less conclusively so.

As always, when one observes Pluto, the effect of Charon must be considered as well. Although the presence of water and the absence of methane on Charon was demonstrated for only one hemisphere (not too far displaced from the April 15 observations), there are two reasons for believing its global spectrum should be free of methane.

The first argument is theoretical, and is discussed in both the previous chapter and in Trafton *et al.* (1988). Due to Charon's relatively feeble gravity, any surface methane should have escaped long ago. Observational evidence, though indirect, also exists. Mutual event observations of Charon both in transit and occultation (Binzel 1988) show that complementary hemispheres of the satellite are spectrally bluer than Pluto, and little color variation is seen throughout the orbit.

Notice that the continuum in the April ratio of phases 0.78/0.94 has a slightly negative slope. We feel this is evidence for variation of color with rotational phase, in the sense that *dark* regions are *redder* than bright regions. If real, this effect is consistent with (but not unique to) the hypothesis that dark regions may be contaminated by the products of methane photolysis and/or bombardment by high energy particles (*cf.* Cheng *et al.* 1986, Cruikshank and Brown 1986, Johnson 1989, and references cited therein). It is known that the dark region causing minimum light has persisted for at least 35 years. To date, theoretical models of seasonal methane migration cannot account for such longitudinal asymmetry.

Binzel (1988) reported little color variation between conjugate hemispheres of Pluto and Charon. Although our tentative result is at odds with his findings, the two results are not necessarily inconsistent. Binzel's observations were limited to the visual region of the spectrum, and were at different rotational phases. However, we do point out that if Pluto is indeed redder at minimum light, this does cast doubt upon his conjecture that, "... the data may be attributed to a direct detection of polar caps on Pluto." If the (bright) polar caps are *bluer* than the mean of all equatorial regions, then at minimum light Pluto's color would be expected to be its bluest, not reddest, for that is when the equatorial regions contribute the least to the integrated global flux. We do point out that the entire problem can be made to disappear if *darker* equatorial regions are *redder* than those low-latitude areas of more moderate albedo.

Clearly, the reddening needs to be confirmed for the longitudes observed, and extended to those regions not yet probed.

There is little evidence in our observations for any variability at either the 1.5 or 2.0 μm absorptions of water. The flux ratio plots show extremely consistent values at wavelengths spanning these two bands for all nights of observation. The Pluto-facing hemisphere of Charon is known to be nearly black at 2.0 μm (Marcialis *et al.* 1987). Let us assume this is a global characteristic of the satellite. One implication is that water frost on Pluto (should any exist at the surface) is likely to be rather evenly distributed, or covered.

4.5. Future Investigation

Although our observations cover 1/3 of Pluto's light curve, investigation into the observed variability in methane and nonvariability in water needs to be extended over the opposite hemisphere. We feel that a similar data set for those regions may provide evidence with which the two existing albedo models of Pluto may be tested. If the albedo/composition trend is a global one, discrimination between the Two Spot Model (TSM) and Twenty-four Parameter Model (TPM) might be within reach.

With infrared array detectors coming into more widespread usage, the multiplexing advantage can be used to increase the spectral resolution, allowing band shapes as well as depths to be measured. This additional information can be used to construct models of methane distribution, and to test those derived from mutual event observations (Buie *et al.* 1989).

Finally, the data presented here serve as a caution to those planning synoptic measurements of Pluto. Some have suggested (*cf.* Cruikshank and Silvaggio 1980, Marcialis 1983, Stern 1984) that as Pluto recedes from perihelion a portion of its atmosphere may condense onto the surface. This should result in a slow evolution in the spectrum over a span of a few decades. Such long-term observations should be planned at a *specific sampling* of representative rotational phases, given the impracticality of detailed observation over the entire light curve. Much care should be devoted to tracking the evolution of continuum slope (color) during this period. Pluto would be expected to become slightly bluer if an optically thick layer of fresh frost coats what is now the surface.

Even then, it must be remembered that the sub-Earth latitude on Pluto currently is varying by approximately $2^\circ\,\mathrm{yr}^{-1}$. The combination of the present results with *either* of the two spot models might actually predict that, over the next decade or two, Pluto's methane absorptions might actually *strengthen* as the northern polar cap swings into view. Without spatial resolution much in excess of that which Hubble Space Telescope will provide, disentangling viewing geometry effects from seasonal ones may prove to be a formidable task indeed.

CHAPTER 5

THE ALBEDOS OF PLUTO AND CHARON: WAVELENGTH DEPENDENCE

The 1987 March 03 occultation of Charon by Pluto was monitored simultaneously with three telescopes in the vicinity of Tucson, Arizona. Each site covered a distinct wavelength interval, with the total range spanning 0.44–2.4 μm. Observing the same event ensures an identical Sun–Pluto–Earth geometry for all three sites, and minimizes the assumptions which must be made to combine results. We have used this spectrophotometry to derive the individual geometric albedos of Pluto and Charon over a factor of ≥ 5 in wavelength.

The contention of Mulholland and Gustafson (1987), that depth and duration of nearly central events "is both wavelength and telescope dependent" is demonstrated to be incorrect. Broader wavelength coverage during a much more central event comprises a test of the hypothesis in accordance with, but more than an order of magnitude more sensitive than, results published by Tholen and Hubbard (1988).

5.1. Background

Mutual events between Pluto and its satellite Charon occur (Andersson 1976) at two intervals per Hadean year, when the Earth passes through the orbital plane of the Pluto system. During these times, the satellite alternatively transits in front of and is occulted behind Pluto once each $6^{\rm d}\!.387245$ days. Each season lasts approximately five years, spaced ~124 years apart. As in the binary star problem, timing of these events has yielded precise radii for the two components (*cf.* Tholen and Buie 1989). Knowledge of these radii, coupled with flux measurements derived from mutual event observations allows calculation of individual albedos for each component. Repetition of the experiment at many wavelengths yields their separate spectra.

Events were predicted to last 5–6 hr. Only rarely could an entire event be observed from a single site. Cooperation between large observatories was essential to detect the initial events, and to ensure maximum coverage once event ephemerides were determined. For these purposes, the Pluto–Charon Mutual Events Season Campaign (PCMESC) was organized at the 1985 Division of Planetary Sciences meeting of the American Astronomical Society. Uniformity of observational techniques, comparison stars choice (at least at visual wavelengths), data reduction, archival, and scientific collaboration in analysis are all stated goals of the PCMESC. This paper represents one of the first such collaborations; no doubt many more are to follow.

5.2. Observations

Data were obtained on UT 1987 March 03 at three telescopes in the vicinity of Tucson, as summarized in Table 5.1. KPNO data (Johnson B and V) appear in Table 5.2 and are plotted as Figure 5.1. The UAO and MMTO observations have been published previously (see Fink and DiSanti 1988, Marcialis *et al.* 1987, respectively). We note that all values in Table 1 of the latter paper (both fluxes and error estimates) are a factor of 2 too large, due to an error in the averaging process.

Telescopes, equipment, and participants in the experiment

Station	Aperture	Detector	wavelengths (μm)	Observers
Kitt Peak	1.27m	photoelectric phot.	B, V	Tedesco, Africano
Mt. Bigelow	1.54m	LPL CCD+spect.	0.4–1.0	Fink, DiSanti
Mt. Hopkins	6×1.82m	MMT InSb phot.	1.5, 1.7, 2.0, 2.35	Marcialis, Rieke

Table 5.1. Multispectral data were obtained at three sites surrounding Tucson.

Taken as a whole, the data span 0.4–2.4 micrometers, nearly a factor of 6 in wavelength. Observation of the same event ensures identical geometry, given the radii of Pluto and Charon are independent of wavelength. Due to differing sensitivities of each telescope/detector combination and decreasing abundance of solar flux with wavelength, it was not practical to use the same comparison object at all three sites. Because of this, there was some concern initially with regard to absolute zero-point calibrations when combining the data. However, all three comparison objects are often-used standards in their respective wavelength regimes, and it appears that each group achieved absolute precision to within several millimag.

First contact occurred shortly after Pluto rose for all sites, which meant that out-of-eclipse flux levels had to be determined at high airmass, and over a time short compared to the event. Outside of event, one observes the sum of flux contributions from Pluto+Charon. During totality (by definition) only Pluto's contribution is seen. Therefore, it is the *out-of-eclipse* observations to which the determination of Charon's contribution are most sensitive.

Morning twilight forced both submicron observatories to terminate observations before fourth contact. Due to the $1/\lambda^4$ dependence of Rayleigh scattering, Kitt Peak B, V observations of Pluto 1987 March 03

UT	V	σ_V	B-V	UT	V	σ_V	B-V
7.36436	13.823	0.010	—	8.89268	13.843	0.007	0.825
7.39947	13.843	0.011	0.827	8.92850	13.850	0.008	0.835
7.44855	13.849	0.014	0.836	8.96444	13.855	0.008	0.841
7.48366	13.830	0.009	0.858	9.05862	13.865	0.009	—
7.58126	13.823	0.013	—	9.09372	13.877	0.007	0.817
7.61636	13.829	0.013	0.834	9.12881	13.879	0.007	0.833
7.65853	13.829	0.012	0.847	9.16390	13.885	0.008	0.865
7.69367	13.831	0.010	0.849	9.20683	13.891	0.009	0.855
7.79081	13.838	0.013	—	9.24192	13.886	0.007	0.830
7.82597	13.833	0.007	0.856	9.27707	13.887	0.007	0.834
7.86683	13.833	0.007	0.865	9.31216	13.894	0.008	0.836
7.90198	13.827	0.007	0.860	9.40232	13.905	0.008	—
7.96770	13.837	0.019	—	9.43747	13.911	0.010	0.851
8.03610	13.831	0.008	—	9.47331	13.908	0.009	0.857
8.10147	13.822	0.009	—	9.50928	13.907	0.011	0.836
8.27691	13.826	0.008	—	9.55340	13.915	0.009	0.835
8.31206	13.841	0.011	0.836	9.58856	13.924	0.011	0.846
8.34715	13.837	0.010	0.836	9.62532	13.935	0.013	0.847
8.38336	13.847	0.008	0.827	9.66051	13.945	0.009	0.839
8.42701	13.842	0.010	0.847	9.75521	13.957	0.012	—
8.46286	13.846	0.010	0.832	9.79028	13.959	0.015	0.839
8.49882	13.845	0.012	0.820	9.82616	13.963	0.011	0.850
8.53391	13.838	0.009	0.841	9.86211	13.974	0.012	0.871
8.61755	13.841	0.009	—	9.90827	13.972	0.012	0.872
8.70890	13.849	0.010	—	9.94417	13.975	0.011	0.854
8.74405	13.847	0.008	0.819	9.98010	13.994	0.014	0.832
8.77913	13.852	0.009	0.833	10.01525	13.976	0.011	0.857
8.81495	13.868	0.013	0.847	10.11148	13.994	0.012	—
8.85754	13.850	0.008	0.837	10.14663	14.000	0.013	0.855

Tabulation continues on following page...

Table 5.2. Reductions of the Kitt Peak 1.27 m Johnson B and V photoelectric observations.

(continued) Kitt Peak B, V observations of Pluto 1987 March 03

UT	V	σ_V	B-V	UT	V	σ_V	B-V
10.18169	13.995	0.014	0.869	11.56764	14.003	0.010	0.849
10.21754	14.005	0.012	0.850	11.61023	14.003	0.012	0.860
10.26174	13.995	0.012	0.859	11.64682	13.999	0.009	0.878
10.29684	13.985	0.013	0.871	11.68290	14.015	0.011	0.854
10.33287	13.985	0.014	0.870	11.71928	14.006	0.012	0.856
10.36898	14.000	0.012	0.866	11.81258	14.002	0.010	—
10.46563	14.010	0.011	—	11.84765	14.004	0.008	0.846
10.50079	14.001	0.010	0.869	11.88380	13.999	0.009	0.846
10.53695	14.006	0.010	0.862	11.91985	13.995	0.008	0.829
10.57302	13.998	0.010	0.891	11.96539	13.988	0.010	0.846
10.61723	13.999	0.010	0.882	12.00214	13.973	0.007	0.864
10.65307	13.995	0.010	0.868	12.03739	13.990	0.010	0.827
10.68913	13.993	0.013	0.854	12.07403	13.965	0.008	0.860
10.72562	14.006	0.011	0.843	12.17169	13.957	0.009	—
10.81022	14.001	0.012	—	12.20844	13.965	0.007	0.824
10.87491	14.018	0.011	—	12.24515	13.949	0.008	0.857
10.96475	14.017	0.015	—	12.28146	13.952	0.007	0.860
10.99987	14.011	0.010	0.837	12.32650	13.956	0.007	0.837
11.03556	14.003	0.009	0.861	12.36300	13.941	0.007	0.835
11.07213	14.022	0.009	0.840	12.39948	13.950	0.007	0.825
11.11529	14.003	0.009	0.876	12.43463	13.943	0.007	0.842
11.15039	14.003	0.009	0.871	12.52621	13.925	0.008	—
11.18673	13.993	0.010	0.885	12.56136	13.916	0.011	0.848
11.22308	14.000	0.008	0.889	12.59742	13.901	0.012	0.871
11.30696	14.002	0.009	—	12.63416	13.909	0.009	0.861
11.37296	14.004	0.009	—	12.67582	13.917	0.008	0.851
11.46027	14.010	0.009	—	12.71232	13.925	0.008	0.828
11.49537	14.010	0.010	0.849	12.74866	13.898	0.008	0.847
11.53171	14.013	0.009	0.845	12.78534	13.900	0.008	0.830

Table 5.2. *(continued)* Reductions of the Kitt Peak 1.27 m Johnson B and V photoelectric observations.

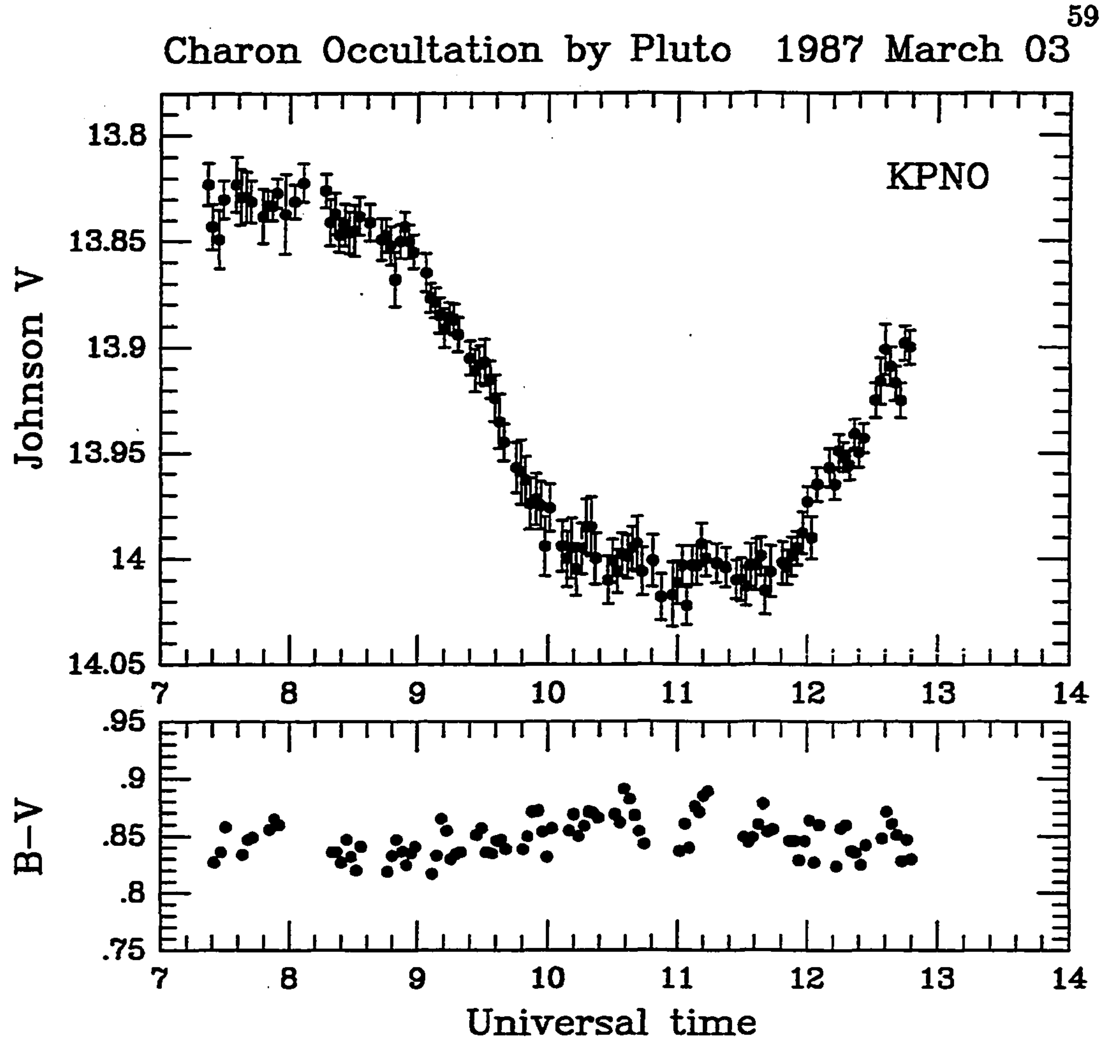

Figure 5.1. Johnson B and V observations of the event, obtained by Tedesco and Africano with the Kitt Peak 1.27-m telescope. Errorbars have been omitted from the $B - V$ data for clarity.

"twilight" occurred much later at the MMT, and it was possible to continue observations there until just minutes before the end of the event. This allows *interpolation*, rather than *extrapolation*, of the out-of-eclipse light curve to its value at mid-event.

The value of interpolation is immediately apparent: linear least squares fits to the B and V pre-event data imply fourth contact brightnesses which are only halfway up the ascending branch of the observed light curve. Extrapolation to mid-event, while only half as severe, still causes spurious results.

To circumvent the problem, ordinates of light curves obtained at B and V were scaled to overlay the 1.5 μm observations. At each color, the estimated brightness at UT 13.133 was determined. Now least squares lines were fit to the out-of-eclipse data, under the constraint that they pass through their respective estimated values at the chosen time. Although the technique is not perfect, any error in the determination of this "synthetic fourth contact" is *halved* when trying to estimate where the light curve would have been at mid-event. In the V passband, we estimate that any error introduced by the application of this artifice amounts to $\leq 0^m\!.002$. Unfortunately, there is no way the poorly determined *pre-event* baseline can be improved upon without additional assumptions, and has resulted in an estimate of the V albedo of Charon which is at odds with the short-wavelength CCD observations.

5.3. Details of Analysis

Accurate absolute flux calibration is critical to the fidelity of an albedo determination; a few percent error in the estimate of the Sun's brightness or color has considerable effect on the results, as we discovered in the initial analysis. The most recent *reliable* Solar values, taken from Campins *et al.* (1985) are believed to be: $V_{\odot} = -26^m\!.762 \pm 0^m\!.017$ (minus sign missing in their paper), $(V-J)_{\odot} = 1^m\!.116 \pm 0^m\!.015$, $(V-H)_{\odot} = 1^m\!.426 \pm 0^m\!.015$, and $(V-K)_{\odot} = 1^m\!.486 \pm 0^m\!.035$. For $(B-V)_{\odot}$, we use Hardorp's (1980) determination of $0^m\!.665 \pm 0^m\!.005$.

The B and V observations were tied in to the "Johnson Pluto system." This system was defined (*cf.* Tholen *et al.* 1987*b*) because the Johnson photometric system is not internally consistent at the millimag level. To calibrate the four infrared light curves we interpolated the JHK colors of both the Sun and our flux standard, HD 129655. For details of the CCD calibrations, refer to Fink and DiSanti (1988).

To calculate the geometric albedo of an object, we start with the fundamental relation

$$p = \frac{\pi I(0^\circ)}{F_{inc}}, \tag{5.1}$$

where p is the geometric albedo, $\pi I(0^\circ)$ is the reflected flux, and F_{inc} is the incident flux from the Sun. The auxiliary relations

$$I(0^\circ) = \frac{F_{meas}\Delta^2}{\pi R'^2} \tag{5.2}$$

and

$$F_{inc} = \frac{\mathcal{F}_\odot}{r^2} \tag{5.3}$$

are substituted to give the more useful final equation,

$$p = 2.23796 \times 10^{16} \times (\text{meas. frac. solar flux}) \times \left(\frac{r\Delta}{R\ [\text{KM}]}\right)^2 . \tag{5.4}$$

Here, $\mathcal{F}_\odot$ is the solar constant, F_{meas} is the absolute flux measured at the telescope, and r, Δ, and R' are respectively the distances from the Sun, Earth, and object radius, in AU; R is the object radius expressed in KM.

The albedo one derives goes as the *square* of both r and Δ. Precise values of these distances therefore strongly influence the calculation. Values were supplied by Mink (Mink *et al.* 1990) from the JPL DE–130 ephemeris; for this event they were 4.44220×10^9 and 4.36443×10^9 km, respectively.

Radii adopted for Pluto (1150±7 km) and Charon (593±10 km) are the most recent values from mutual event analysis (Tholen and Buie 1989). Alternatively, the slightly larger (2σ) radius determination for Pluto from the recent stellar occultation (Hubbard *et al.* 1988, Elliot *et al.* 1989) could have been used.

In their nonisothermal atmosphere model of this event, Hubbard *et al.* (1990) quote a likely radius for Pluto in the vicinity of 1180 km. This determination is 2.6% *larger* than the value derived from the mutual events. A decade ago, Walker (1980) observed a stellar occultation by Charon which lasted 50 sec, implying a *minimum* radius for Charon of 600 km, again larger ($\geq 1.2\%$) than the mutual event determination. The fundamental unit of distance in mutual event analysis is the satellite's orbital semimajor axis a, which must be determined independently for an unresolved binary. The Tholen model uses speckle interferometry by Beletic *et al.* (1989) to assign a value of $19,640 \pm 320$ km to a. Should this be an underestimate of the true value by, say, 2.6%, then both the mutual event and occultation solutions become consistent, and the albedos derived here should be revised *downward* by $(2.6)^2$ %, or $\sim$6.8%.

It is expected that imaging by the Hubble Space Telescope soon will make a direct determination of the system "yardstick" to resolve the matter. In any case, application of Equation (5.4) makes future recalculation rather trivial.

As the separate phase functions for Pluto and its satellite have not yet been determined, no correction was made for the opposition effect. However, the defect of illumination due to the instantaneous solar phase angle (1$^\circ\!\!.$64) tends to lower the albedos which result from application of Equation (5.4). This correction amounts to only 0.02%, but has been taken into account nevertheless. Clearly, the contributions from "Pluto-shine" and "Charon-shine" may be neglected.

5.4. Results and Interpretation

Figure 5.2 plots the instantaneous albedos for Pluto and Charon as a function of wavelength, based solely on the 1987 March 03 event. We emphasize that these values are hemispherical averages. Since the out-of-eclipse lightcurve slope is apparent during totality, we know that the albedo of Pluto's surface varies with rotational phase. The combined light of the system undergoes peak-to-peak variation of $\sim$0$^m\!\!.$30 as the planet rotates each 6$^d\!\!.$387245. Totality slopes at continuum wavelengths tend to be as large as, or marginally larger than, out-of-event values. This is what would be expected if Pluto were the dominant contributor to the system light curve. Charon's flux contribution only serves to "dilute" the overall lightcurve variation. From the observations reported here and by others (Binzel 1988), it appears Charon's surface is rather uniform in albedo at any given wavelength.

We note that the logbook for the Kitt Peak site reads, "Sky clear at start of night except for thin cirrus on western horizon. Clear at end." Photometrists are well aware that such clouds are much more easily seen against the backlit sky of twilight than under different conditions. Let us now assume, purely for the sake of argument, that a thin layer of cirrus was present during the very earliest observations, and that it had totally dissipated by the start of the event. The first few measurements were made at a (usually unacceptable) high airmass, $X \gtrsim 2$, when they were most susceptible to temporal and/or spatial variations in the extinction

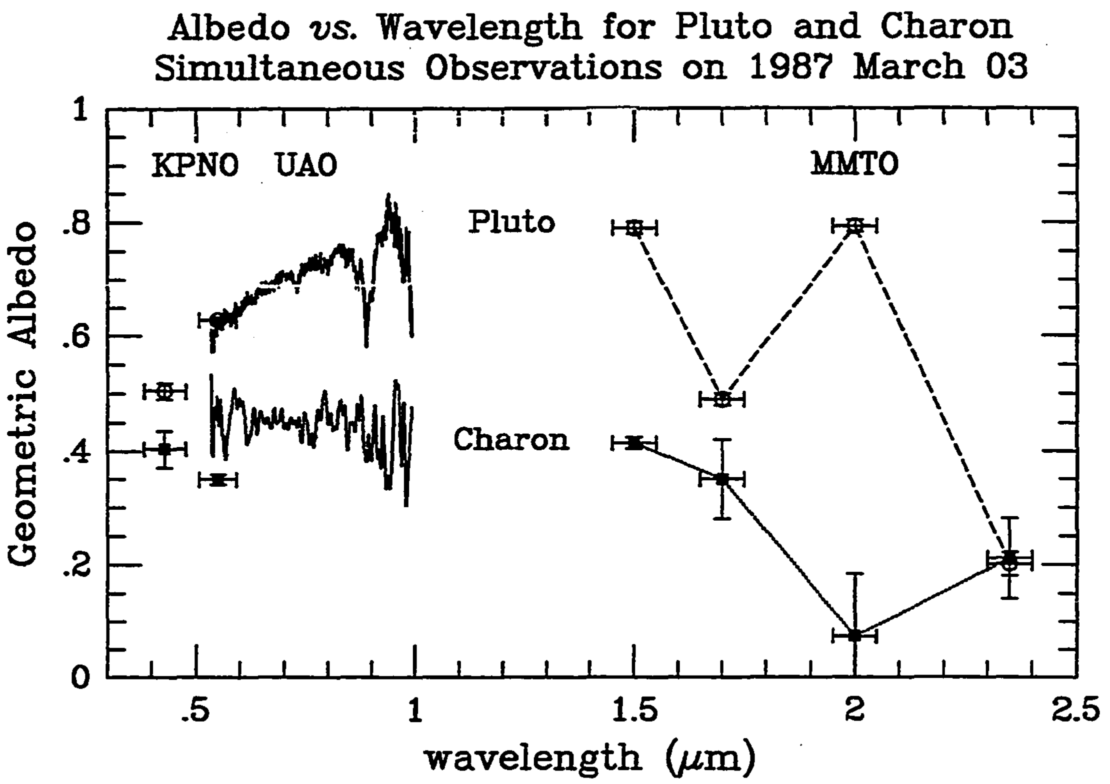

Figure 5.2. Mean hemispherical geometric albedos for Pluto and Charon, as a function of wavelength. For the filter photometry, horizontal bars indicate the FWHM bandpasses. The CCD spectrum of Pluto is shown at the full original resolution of 12 Å pixel^{-1}, while Charon's spectrum has been smoothed to suppress internal variations less than 15 pixels wide. Insufficient pre-event coverage at high airmass, as well as thin cirrus noted in the logbook at sunset, probably are responsible for the low estimate of Charon's albedo at *V*.

coefficient. If we work under the assumption that at pre-event (Pluto+Charon) actually was just $0^m\!.02$ (1%) *brighter* than the data show, the *V* albedo derived for Charon is affected considerably. (The *B* data are noisier, with mean error comparable to this "correction" in any case, and computed p_B's are essentially unchanged.

Exclusion of the two faint "outliers" at about 7:15 UT can account for much of this proposed 2% discrepancy. Reworking the problem, we now find (Figure 5.3)

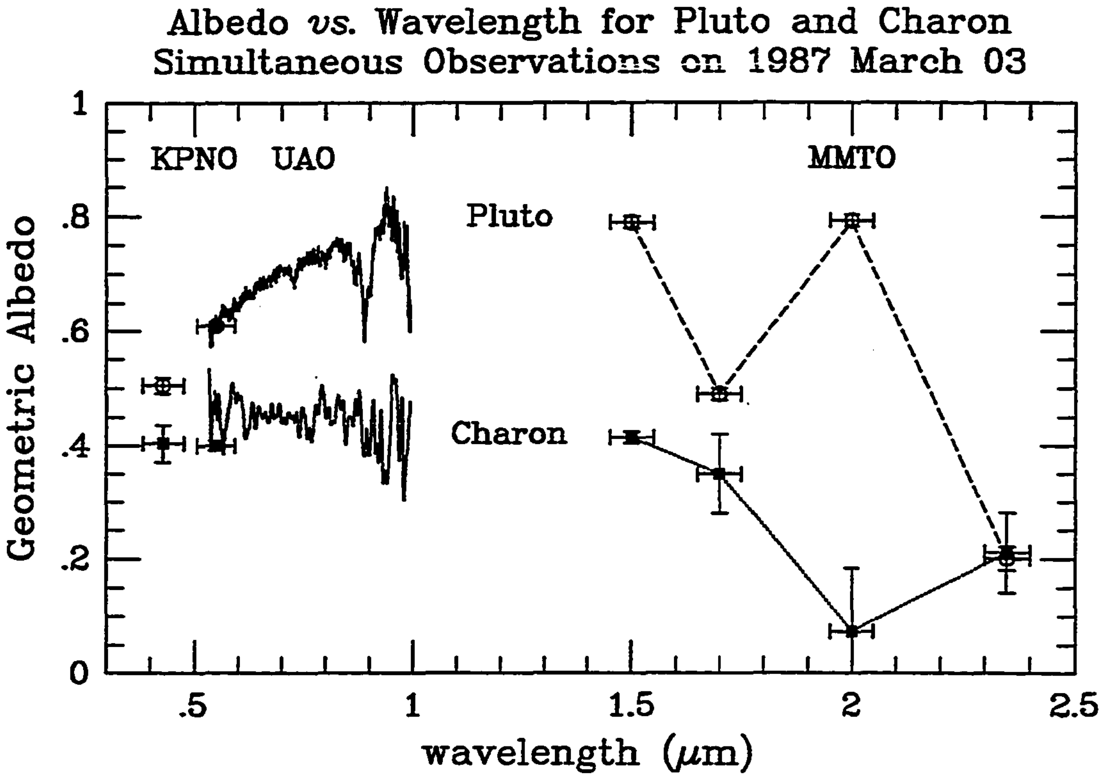

Figure 5.3. Under the assumption that the pre-event combined light of Pluto + Charon was actually 2% *brighter* than the data show, the Kitt Peak and UAO V geometric albedos derived become much more consistent.

the calculated geometric albedo of Charon is raised to a value of $p_V = 0.40$. The Kitt Peak data now are totally consistent with the UAO spectra.

All absorptions in the spectrum of Pluto may be attributed to methane (*viz.* 2.35, 1.7, 0.89, 0.72 μm). Pluto's continuum slope in the visible rises toward the infrared, peaking somewhere between 0.95–1.5 μm at a rather large value of ~0.8. Remember that at maximum light the combined Pluto–Charon light curve is ~8% brighter, meaning that the hemispherically-averaged peak albedo of Pluto must approach 90%. Other solid-surface bodies in the solar system bodies have geometric albedos comparable to, or greater than, this value, but in the visual.

Saturn's Enceladus (water frost on surface, $p_V > 1$) and Neptune's Triton (surface frosts of methane and nitrogen, $p_V = 0.78$; *cf.* Smith *et al.* 1989) are two notable examples. However, neither of these bodies have surfaces as "red" as Pluto's.

In Chapter 4 (Marcialis and Lebofsky 1990) we report evidence from 1.0–2.5 μm spectrophotometry that albedo and composition on the surface of Pluto appear to be correlated. Bright regions are enriched in methane relative to dark, and there is at least preliminary evidence that dark regions tend to be redder than bright regions. UV photochemistry and bombardment by high-energy particles each are known to darken and redden laboratory samples of methane (Lunine *et al.* 1989, Cheng and Johnson 1989).

That such considerable longitudinal variation should exist on Pluto (where it has persisted for four decades) but not on Triton may be diagnostic of the relative abilities of these two icy surfaces to "launder" themselves *via* seasonal migration of their surface layers (see Stern *et al.* 1988). Alternatively, Pluto may have a spectrally-red surface component, not derived from its methane inventory, which Triton lacks. In either case, clearly something is different about the surface environments of these two bodies, so often considered to be virtual "twins" in the outer solar system.

As reported in Chapter 1, Charon appears devoid of surface methane. The deep absorption seen at 2.0 μm comprises the discovery observation of water frost on the satellite (Marcialis *et al.* 1987). Higher resolution spectrophotometry "confirming" this feature subsequently was obtained by Buie *et al.* (1987). However, those data have not been included in Figure 5.2 for two reasons. First, the geometry was different; second the deviation of the Buie *et al.* data from *flat* continuum is only marginally significant (reduced Chi-squared, $\chi^2_r = 1.06$), and totally insignificant if slope is allowed to be a free parameter.

Charon's slightly blue continuum appears to retain a constant slope out to $1.5\,\mu$m, with albedo decreasing at the rate of $\sim$5.2 percent micron^{-1}, about twice as large as the value initially reported by Fink and DiSanti (1988). Except at the core of the deep $2.35\,\mu$m absorption of methane, Charon is consistently darker than Pluto.

5.5. Absence of Diffraction Effects

Mulholland and Gustafson (1987) suggested that both depth and duration of nearly central Pluto–Charon mutual events might show considerable dependence on both wavelength and telescope aperture. Tholen and Hubbard (1988) offered a subset of data obtained over six months in 1986 (all partial events, at 0.44 and $0.55\,\mu$m) which show no evidence for such diffraction effects.

The observations reported here are in accordance with what Tholen and Hubbard report. However, our broader wavelength coverage (factor of $\gtrsim 5$) *was obtained during a single, total event.* The experiment comprises a much more stringent test of the original hypothesis. Many combinations of aperture/wavelength ratio, $\lambda/d \geq 2$, were tested simultaneously, in an experiment where geometry was *identical.* We find that none of these combinations has any effect whatsoever upon event duration, and demonstrate that the only effects on event depth may be attributed purely to differences in surface composition (*i.e.*, albedo) between planet and moon.

CHAPTER 6

TOPOGRAPHIC RELAXATION ON ICE-COVERED WORLDS: APPLICATION TO PLUTO

The subject of topographic relaxation into a methane "lithosphere" is addressed. It is assumed that an empirical temperature-viscosity law for water ice, when restated in terms of melting temperature, will provide an upper-limit for the rheologic behavior of methane ice. The approach of Parmentier and Head (1979) and models of Pluto's interior based on mutual event data are used to show that the planet is incapable of supporting lateral topography of characteristic scale $\gtrsim$ 10 km for the age of the solar system. Globally, Pluto's figure is expected to be essentially hydrostatic.

6.1. Introduction

The subject of topographic relaxation through viscous flow has been addressed several times over the past 50 years. Most previous studies have dealt with rocky lithospheres, or lithospheres composed predominantly of H_2O ice at absolute temperature $\gtrsim$ half the melting point (*cf.* Haskell 1935, 1936; Scott 1967; Parmentier and Head 1979, 1981; Parmentier *et al.* 1980). Marcialis (1985, 1989*a,b*) undertook the first investigations of topographic relaxation into a methane lithosphere. The purpose of the present paper is to summarize those preliminary calculations, and to update them in light of the recent, more realistic interior models of Pluto which have resulted from analysis of the present series of Pluto–Charon mutual events.

This treatment is intended only as a first step in the development of the subject; substantial laboratory work will be required to verify the validity of the assumptions made. In this paper the lack of engineering data is circumvented through use of scaling law arguments to predict a theoretical creep law for methane. Additionally, processes besides solid-state creep, such as mass wasting, sublimation, photolysis, and exo- or endogenic seismicity are neglected, and can only serve to speed the settling or erosion of surface features. Nonetheless, it is hoped that our results will prove to be at least a reasonable upper bound to actual topography on the planet.

6.2. Interior Structure of Pluto

Before we can investigate viscous relaxation on Pluto, we must first have an interior model for the structure of the planet, at least in the "near field" of any topographic features.

A theoretical study by Lupo and Lewis (1980*a, b*) was for a decade the only published study of the interior structure and composition of the planet. Recently, more realistic models of Pluto's interior have appeared as a result of the mutual event analysis (*cf.* Simonelli *et al.* 1989, Simonelli and Reynolds 1989, McKinnon and Mueller 1988). The bulk density of Pluto/Charon, about $2.030\,\mathrm{gm\,cm^{-3}}$ (Tholen and Buie 1989), is much higher than was expected before the acquisition of mutual event data. Obviously, the methane mass fraction is smaller than previously believed, and any methane lithosphere must also be correspondingly thinner.

Figure 6.1 depicts Pluto in cross-section, based upon the aforementioned models. Only the outermost regions are of consequence to this study. The topmost layer (the methane "lithosphere") is $20 \pm 10\,\mathrm{km}$ in thickness (liberal error bar estimated from Simonelli paper). Beneath is a mantle of water ice. The rather low thermal conductivity of methane manifests itself in a thermal gradient of about 0.6 °K km^{-1}. Assuming a surface temperature of about 55 °K, and a core with a specific heat production of $\sim 4 \times 10^{-8}$ erg gm^{-1} sec^{-1} (roughly chondritic), integration of the equation of heat flow shows this layer is not solid at the base if it is modelled as purely conductive. Convection is expected to be the dominant means of heat transfer at the bottom of the layer. Some important physical properties of methane ice appear as Table 6.1.

Physical properties of methane ice

Quantity	Value
Equation of State	$\rho = 0.5281 - 2.832 \times 10^{-4} \times T + (2.9655 \times 10^{-5} - 1.709 \times 10^{-9} \times P) \times P$
Coeff. of thermal expansion	$\alpha = -2.832 \times 10^{-4}$ °K^{-1}
Heat capacity	$C_p = 5.5 \times 10^6 + (3.66 \times 10^5 - 1.4 \times 10^3 \times T) \times T$
Thermal conductivity	$K = 24,790 + (708.3 + 7.803 \times T) \times T$
Melting point	$T_m = 90.65$ °K
Boiling point	$T_b = 111.65$ °K

Table 6.1. Physical properties of methane ice. All units cgs, except P in bars. From Lupo and Lewis (1980*a*) and *CRC Handbook*.

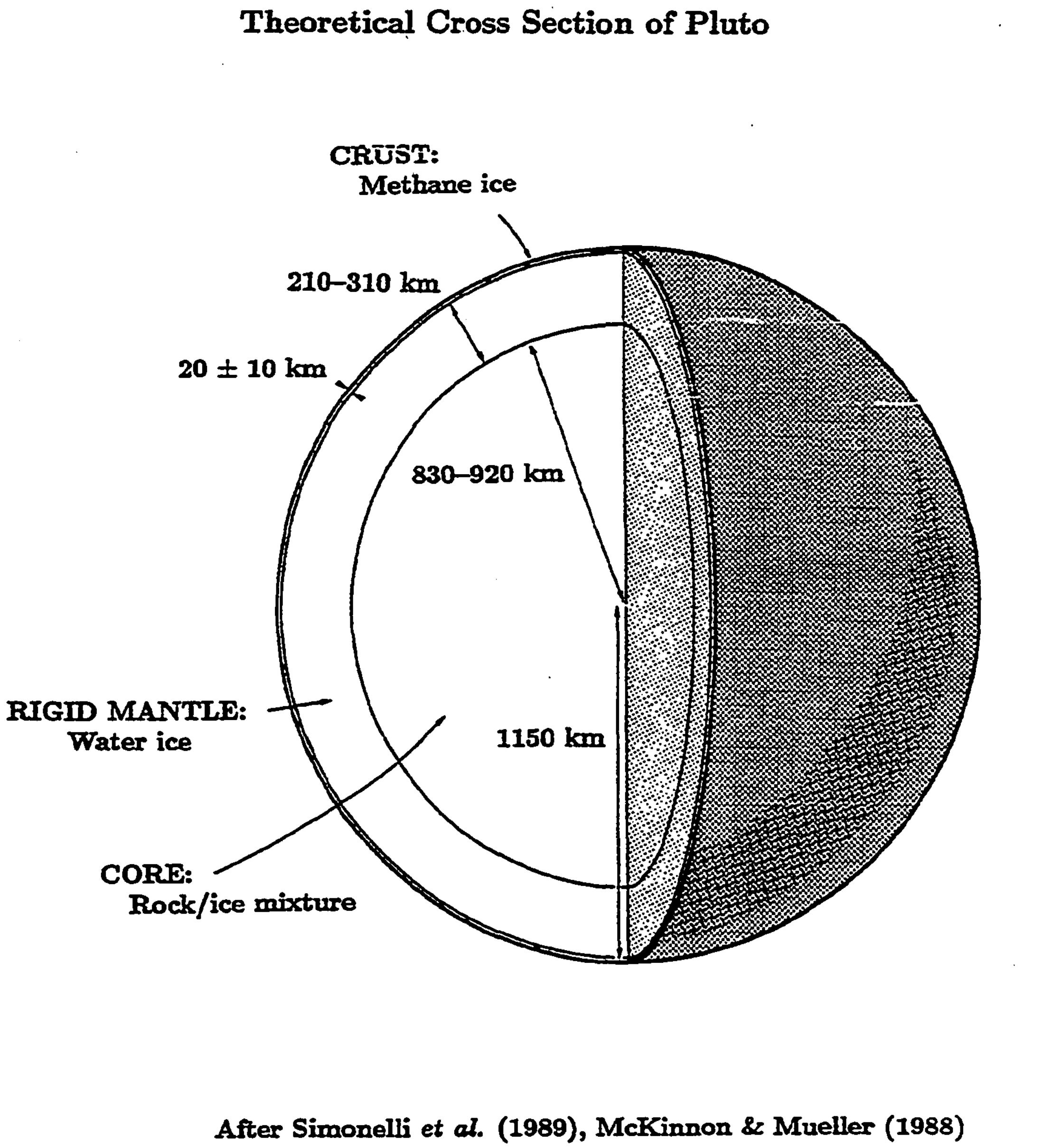

Figure 6.1. Theoretical cross-section of Pluto, after the models of Simonelli & Reynolds (1989) and McKinnon & Mueller (1988).

It is expected that pure CH_4 is the stable species, as opposed to methane clathrate hydrate ($CH_4 \cdot nH_2O$). Consolmagno and Lewis (1978) claim clathrates are unstable at high pressures (the lattice holes disappear), and subsequent differentiation will result in layers of water and methane. Even were clathrates the original species, their extremely low thermal conductivity virtually ensures a radial temperature gradient steep enough to result in eventual differentiation of the layer, from the bottom on up.

The water ice layer should behave as a rigid half-space, at least when compared to the methane veneer. This is because the temperature at the interface is a large fraction of methane's melting point, but still less than $1/3$ of water's melting temperature.

6.3. Methane Rheology

To first order, it is assumed that both methane and water ice behave as Newtonian fluids. That is, the strain rate $\dot{\epsilon}$ is given by

$$\dot{\epsilon} = \frac{\sigma}{\eta}, \tag{6.1}$$

where σ is the applied stress, and η is the viscosity. It is assumed that the strain rate follows an Arrhenius relation,

$$\dot{\epsilon} = B(\sigma) \exp\left\{ - \text{const}\, E^{*} \left(\frac{T}{T_m} \right) \right\}. \tag{6.2}$$

The exponent in the Arrhenius relation is composed of three terms: an "activation energy" (energy required to initiate a dislocation in the crystal lattice), temperature (expressed in units of the melting point temperature T_m), and a constant of proportionality. The utility of this relationship has been verified for many materials. Thus the viscosity of solids deforming through steady-state creep can be expressed as

$$\eta = \eta_m \exp\left\{A\left(\frac{T_m}{T} - 1\right)\right\} , \tag{6.3}$$

if η_m and T_m are respectively the viscosity and temperature at the melting point. The constant A is nominally between ~18 and 26. Ellsworth and Schubert (1983), following Schubert *et al.* (1981) and Hughes (1976) find the viscosity of water ice to be well-approximated by

$$\frac{\eta}{\rho} \equiv \nu = 1390 \exp\left(7214/T\right)\ \mathrm{cm}^2\,\mathrm{sec}^{-1} . \tag{6.4}$$

(An article by Poirer (1982) reviews the rheological properties of water ice as it applies to the outer satellites.) Equation (6.4) may be rewritten in terms of the homologous temperature, $\Theta\ (\equiv T/T_m)$,

$$\nu = 1390 \exp\left\{\frac{26.41}{\Theta}\right\}\ \mathrm{cm}^2\,\mathrm{sec}^{-1} . \tag{6.5}$$

This is actually an *upper limit* for the viscosity of methane ice, since Van der Waal's forces in $H_2O \gg CH_4$ due to the symmetry of the CH_4 molecule (no hydrogen bonding). An admixture of silicates can greatly augment the strength of an ice. Meteoritic influx is one such source of material, above and beyond whatever impurities may remain entrained in the methane since accretion. Thus the actual surface of Pluto may be somewhat "stiffer" than pure CH_4, but by using a viscosity-temperature relation derived from that of H_2O at least partial compensation for this possibility is included in the model.

6.4. Model

The model we choose is exactly that of Parmentier and Head (1981), *i.e.*, a viscous surface layer underlain by a rigid substrate. In the viscous layer, the temperature gradient is assumed to be linear with depth, which by Equation (6.5) implies that viscosity decreases exponentially with depth. The *e*-folding distance for viscosity can be expressed in terms of the geothermal (hadesthermal?) gradient β and surface temperature T_o as:

$$\frac{1}{L} = -\frac{d}{dz}\left\{\ln\frac{\eta}{\eta_o}\right\}\bigg|_{z=0} = \frac{A(T_m - T_o)\,\beta}{T_o^2}\,. \tag{6.6}$$

Recall that the constant $18 \lesssim A \lesssim 26$. The upper value is used for purposes of calculation, but any uncertainty introduced by the precise choice of A is in any case less than that in our estimate of the methane layer thickness.

Relaxing topography may be represented as a time-variant superposition of harmonics, each of which independently decays in a time characteristic of that wavelength. The relaxation time is a function only of wavelength if the layer thickness and viscosity-depth variation are specified. The model is depicted schematically in Figure 6.2, and the assumed and derived parameters relevant to this model appear in Table 6.2. For simplicity we assume topography with circular symmetry (*e.g.*, craters) which may be described as an infinite sum of weighted Bessel functions.

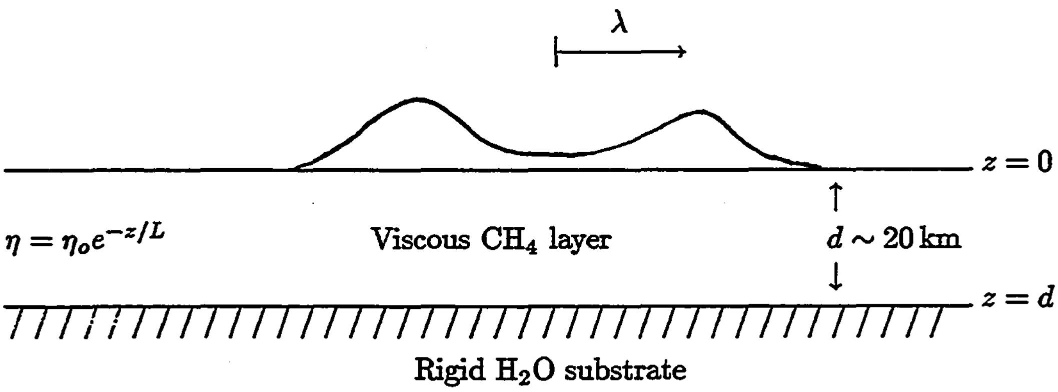

Figure 6.2. Model for the relaxation of topographic features on Pluto. An infinitely rigid half-space of water ice is overlain by a methane ice "lithosphere." The methane has a linear thermal gradient, and therefore an exponentially decreasing viscosity-depth dependence.

Relevant parameters for methane layer

Quantity		Value	
mean density	$\bar{\rho}$	0.54	gm cm^{-3}
surface gravity	g	65.9	cm sec^{-2}
thickness of CH_4 layer	d	20 ± 10	km
viscosity scale height	L	57	km
surface temperature	T_o	55	°K
surface viscosity	η_o	6.02×10^{-21}	gm cm^{-1} sec^{-1}

$\Rightarrow L/d \sim 0.27^{+0.27}_{-0.09}$

$\Rightarrow \frac{\rho g d}{\eta_o} \sim 7.38 \times 10^{-7}\ \mathrm{yr}^{-1}$

Table 6.2. Parameters assumed for the Pluto model depicted in Figure 6.2.

It is assumed that the horizontal extent of topography greatly exceeds its vertical extent. Simply stated, slopes are small. Batchelor (1967) gives the equations of mass conservation and viscous flow for an incompressible fluid in which motions are slow enough that acceleration terms may be neglected. Let h be the topographic height measured from the reference level $z = 0$. For boundary conditions, we require that hydrostatic normal and vanishing shear stress at this level be given by $\sigma_{zz}|_{z=0} = \rho g h$ and $\sigma_{xz}|_{z=0} = 0$, respectively. For details of solution, see Parmentier and Head (1981). Their Figure 1 forms the basis of our results for Pluto. It plots (in our notation) $\rho g d \tau / \eta_o$ *vs.* kd, where τ is relaxation time, η_o the viscosity at the surface, and k is the topographic wavenumber ($= 2\pi/\lambda$). All that remains to be done is to evaluate each parameter appearing in this nondimensional plot.

6.5. Results

Figure 6.3 illustrates graphically the results of our model for methane layers of 10, 20, and 30 km thickness. It is unlikely that topography of lateral wavelength scale $\gtrsim$ 5 km can persist on the surface of Pluto for the age of the solar system; *e*-folding times are under 1 Gyr, even for the most extreme model assumptions. Relaxation time can be as short as 100,000 yr for features in the ~50 km range. Within the assumptions of the model, the existence of features from 10's to 100's of km implies either a relatively recent origin, or a markedly thinner methane layer than currently is believed to exist.

It should be mentioned that N_2 frost, due to its lower melting temperature (63 °K) and higher vapor pressure, is expected to be structurally weaker than CH_4. Efforts to detect nitrogen on Pluto have proven unsuccessful (Cruikshank, personal communication). However, Voyager 2 dispelled all doubt of its presence on Triton, both in solid and gaseous forms. Both nitrogen and methane previously had been detected from Earth (*cf.* Cruikshank *et al.* 1989).

Compared to Pluto, Triton is slightly larger ($R = 1350 \pm 5\,\text{km}$), has essentially the same density ($\rho = 2.075 \pm 0.019\,\text{gm}\,\text{cm}^{-3}$) and has a cooler surface temperature (37 °K). Nevertheless, it is the closest analog to Pluto in the solar system. Quoted values are from Smith *et al.* (1989), who state, "... impact craters generally are rare ... Larger craters, ranging up to the largest (27-km diameter) are complex, having flat floors and central peaks." This is entirely consistent with our results, as the homologous temperatures for nitrogen on Triton and methane on Pluto are identical to within ≤4%. Hence, Triton is the closest "real world" test of the current calculations we will have for many years.

Briefly considering CO ice, which has not been detected on either Pluto or Triton, we remark that it has an even lower melting temperature than N_2. One would expect CO to be even less structurally competent than N_2 or CH_4. However, the strong ionic bond between carbon and oxygen will, no doubt, boost its stiffness in the crystalline state (activation energy for crystal dislocation $\gg$ CH_4 or N_2). We state that the scaling laws used in this paper should not be trusted when applying the current treatment to hypothetical planets having a crustal component of carbon monoxide ice.

6.6. Conclusions

The present results are nearly the same as those obtained by Marcialis (1985) when using the less-dense, pre-mutual event interior models of Pluto. Although the methane layer is thinner than what was assumed for that preliminary study, the surface gravity is higher as well (it scales linearly with bulk density). Since the ordinate of Figure 6.3 is proportional to the product of surface gravity and methane layer thickness, it is rather insensitive to the small uncertainties in

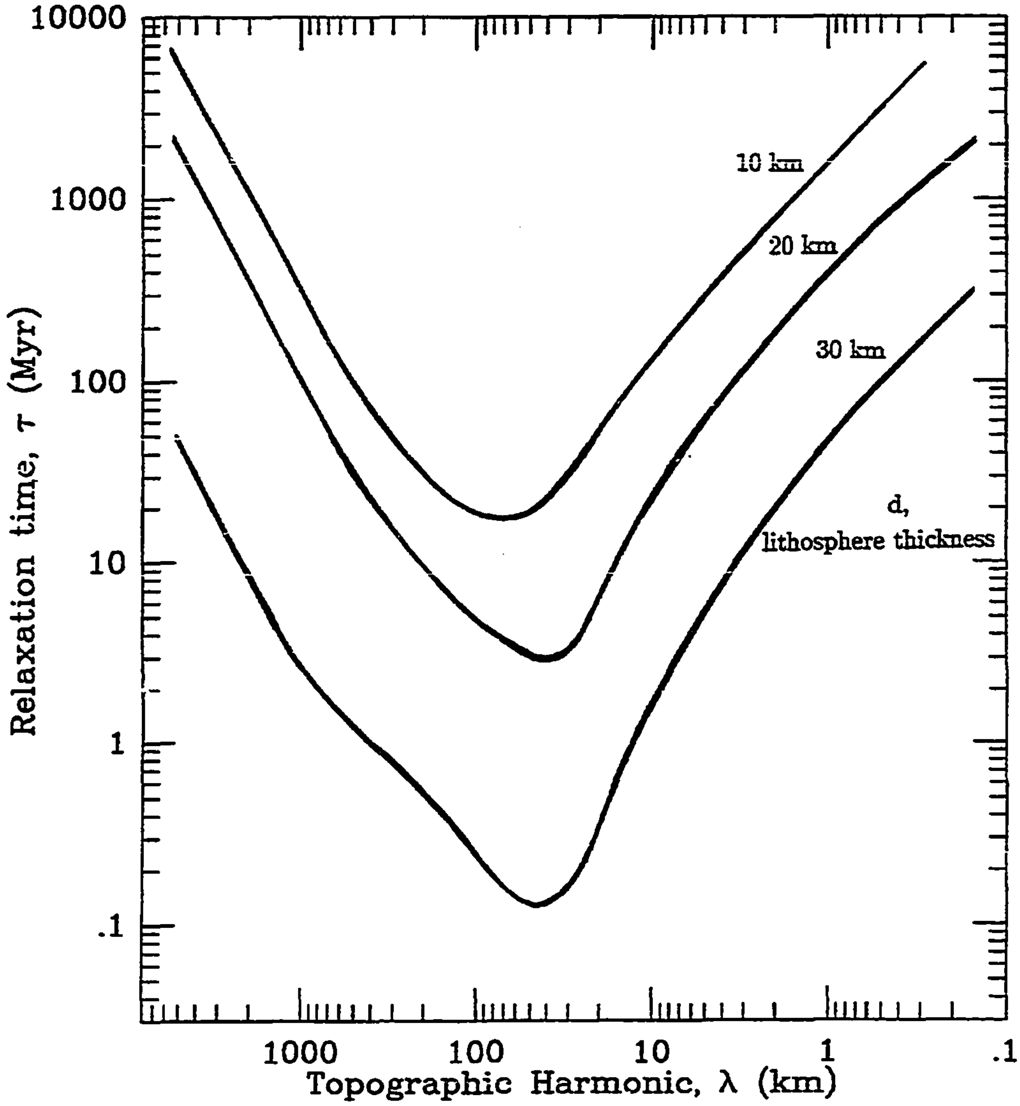

Figure 6.3. Plotted is the *e*-folding time for relaxation of topographic features, as a function of characteristic wavelength harmonic. The calculation has been repeated for three different assumed thicknesses of Pluto's methane layer.

estimates of planetary radius (< 50 km) or mass (< 5%) being bandied about at present.

On a global scale, Pluto's figure is expected to be essentially hydrostatic, with deviations from sphericity being wholly attributable to the superposition of rotational and tidal potentials (the latter being due to its satellite Charon). The deviations amount to ~0.32 and ~0.12 km, respectively. One implication is that only about 1 millimag of the system's ~300 millimag light curve may be attributed to Pluto's shape. Clearly, a distributed albedo is the dominant contributor (see Marcialis 1988*a*).

Methane is conspicuously absent on the surface of Charon, whose spectrum (Marcialis *et al.* 1987; see Chapter 2 and 5) is consistent with a mixture of water frost and a dark, nearly neutral absorber. Should some future flyby mission come to pass, images would most likely reveal surfaces which are markedly different on the two bodies. Under the assumption that both bodies emerged from the period of heavy bombardment gravitationally bound (*i.e.*, sharing a common positional history in the solar system), comparison of crater statistics could tell much about the subsequent cratering history in the vicinity of 30–50 AU. Such a comparison, coupled with laboratory measurements of creep in methane ice, would supply further constraints on the thickness (and global isotropy) of Pluto's surface layer.

CHAPTER 7

ASTROMETRIC OBSERVATIONS OF PLUTO: 1965–1981

This chapter presents photographic astrometric observations obtained between 1965 and 1981 of the planet Pluto. Most of the positions were measured for the purpose of refining the ephemeris of Pluto. This ongoing project is useful in that it allows potential stellar occultations by Pluto to be more accurately predicted, and may also aid in the search for a tenth planet (*cf.* Van Flandern *et al.* 1981).

All observations have been made with the 61 cm Seyfert reflector of the A. J. Dyer Observatory in its reflector-corrector configuration (Seyfert 1956). Direct photographs, one exposure per plate, were taken either on Kodak IIaO or IIaG emulsion. Reference stars were taken from the AGK3, FK4, or SAO catalogs. Each plate covers about 4 deg^2 on the sky (plate scale 100 $\mathrm{arcsec\,mm}^{-1}$) and includes 10–20 reference stars. The plates were measured with the USNO's Semiautomatic Measuring Machine (SAMM) (Harrington and Mintz 1972) and reduced using a standard algorithm kindly supplied by R.S. Harrington. Based upon analysis of the reference stars, the mean positional errors are about 0.5 arcsec in both right ascension and declination.

The positions in Table 7.1 are topocentric right ascension and declination for the equinox 1950.0. Mean epoch of observation is Coordinated Universal Time (UTC) for each exposure.

Astrometric positions of Pluto photocenter

U.T. Date			R.A. (1950.0)	Dec.
1965	November	30.46806	$11^h39^m47\overset{s}{.}54$	$17°53'46\overset{''}{.}1$
1965	November	30.47639	$11^h39^m47\overset{s}{.}61$	$17°53'45\overset{''}{.}9$
1965	November	30.48333	$11^h39^m47\overset{s}{.}64$	$17°53'46\overset{''}{.}1$
1966	December	19.47153	$11^h49^m01\overset{s}{.}34$	$17°25'27\overset{''}{.}1$
1967	February	08.38194	$11^h47^m37\overset{s}{.}75$	$17°59'40\overset{''}{.}0$
1967	February	08.40625	$11^h47^m37\overset{s}{.}58$	$17°59'41\overset{''}{.}9$
1968	March	01.27465	$11^h54^m40\overset{s}{.}04$	$17°40'28\overset{''}{.}6$
1968	March	01.35451	$11^h54^m39\overset{s}{.}62$	$17°40'31\overset{''}{.}7$
1968	March	02.29028	$11^h54^m34\overset{s}{.}39$	$17°41'15\overset{''}{.}3$
1970	April	05.25278	$12^h09^m13\overset{s}{.}63$	$16°44'58\overset{''}{.}1$
1971	May	22.12743	$12^h14^m42\overset{s}{.}73$	$16°11'48\overset{''}{.}4$
1971	June	25.11076	$12^h14^m18\overset{s}{.}10$	$15°57'17\overset{''}{.}9$
1972	March	15.29167	$12^h29^m18\overset{s}{.}92$	$15°07'06\overset{''}{.}6$
1972	April	19.18681	$12^h25^m56\overset{s}{.}27$	$15°26'45\overset{''}{.}1$
1973	March	06.29792	$12^h39^m14\overset{s}{.}94$	$14°14'27\overset{''}{.}5$
1981	March	09.28542	$13^h52^m35\overset{s}{.}20$	$07°15'59\overset{''}{.}3$
1981	March	10.29583	$13^h52^m31\overset{s}{.}02$	$07°16'46\overset{''}{.}9$

Table 7.1. Final reductions of plates obtained at the A.J. Dyer Observatory.

CHAPTER 8

THE DISCOVERY OF CHARON: HAPPY ACCIDENT OR TIMELY FIND?

It is argued that the discovery of Pluto's only known satellite was not serendipitous, but rather an event whose time had come. The 1960s through 1980s represented an era when both geometry was favorable and technology available to allow the find to occur. The 1978 discovery happened nearly at the midpoint of the interval when discovery probability was at its highest.

8.1. Introduction

It is often heard, both at professional meetings and informal gatherings, that the discovery of Pluto's satellite Charon (1978 P1) was one of the luckier findings of the past few decades for planetary astronomy. The discovery, by James Christy and Robert Harrington of the United States Naval Observatory (1978), came a scant ten years before the 1988 passage of the Earth through the orbital plane of the satellite. This passage has resulted, since 1985, in the nearly completed season of eclipses, transits, and occultations (hereafter, mutual events). These mutual events have yielded more concrete results about the Pluto–Charon system in the past three years than was learned about the ninth planet since its discovery by Clyde Tombaugh in 1930. It is the intention of this paper to try to demonstrate that the discovery time, coming only 3% of an orbit before the mutual event season, was *not* fortuitous. Rather, it was the natural result of the concurrent ripening of technology and Pluto's favorable viewing geometry as seen by earthbound observers. In this paper are recounted the advances in instrumentation and observing technique (which impose an early bound to the discovery), and the several characteristics of both Charon's orbit about Pluto, and their mutual heliocentric orbit, which place a latter bound on the most likely time of discovery. It was almost exactly at the middle of this twenty-odd year period that James Christy noticed a bump circulating around Pluto's image.

8.2. Technological Advances (a pre-1965 limit)

There were three major advances in the science of astrometry which had to occur before Charon could have been detected. These three are all intertwined, coming about as a result of each other. Two concern the hardware used in obtaining astrometric data; the third was a result of the increased sensitivity afforded by the equipment introduced in the mid-1960s.

The 1964 completion of the USNO 155-cm reflector in Flagstaff, Arizona marked the beginning of a new era for astrometry (Strand, 1971). It was significant in that it hailed the introduction of large reflecting telescopes to astrometrical problems, a field previously the domain of the classical long-focus refractor. The greater light-gathering ability of a large mirror allowed plates to be exposed for shorter times with the same results. These shorter exposures resulted in narrower point-spread functions for stellar images, *i.e.*, turbulence in the atmosphere had less time to statistically "smear out" the image of a star. Although the existence of this telescope was, in and of itself, not a requirement for the discovery of Charon, it *did* cause astrometrists to rethink their procedures as to plate reductions.

A simultaneous advance in the field of astrometry was the introduction of automated measuring engines. Milestones in this area were the SAMM and

GALAXY machines (Strand, 1966; Dodd, 1972; Riddle and Worley, 1966). The additional speed afforded by automating the previously tedious process of plate mensuration allowed a marked increase in the productivity of a given facility: the locations of many more objects could be monitored without producing a backlog of unreduced plates. In addition to being faster at measuring plate positions, these machines afforded greater positional accuracy than was possible previously. Profiles of stellar images could be determined analytically, and centroids of individual point-spread functions determined to better than a micrometer—a distance much smaller than the actual image size recorded on the photographic emulsion.

Increased accuracy of measurement induced the third—and probably most significant—modification to observing techniques (Christy, 1987; personal communication). When manual determination of the center of a stellar image was the norm, plates traditionally were overexposed. Although this saturated the cores of the stellar images, it tended to "smear out" the wings, providing large, round images whose centers the human eye could then determine. When measuring engines had advanced to the point of fitting image profiles, say, as the sum of gaussians, it was found that such fits became more accurate if the cores of the images were not saturated, but rather more properly exposed in the linear regime of the photographic emulsion. Once exposure times were cut down, it was then possible to resolve many binaries—both for stars, and in the case of Pluto, for a planet—that had previously been "burnt in" to the emulsion as a single source. This explains the failure of Humason's 1950 Plutonian satellite search using the 200-in Palomar telescope (Kuiper, 1961). With the shorter exposures, I have seen the asymmetry which is Charon on images taken with as small a telescope as the 61-cm Seyfert reflector of the A. J. Dyer Observatory (Hardie *et al.* 1984).

The combined effects of the above three innovations were such that the technology required to discover a faint, close-in ($m_V \sim +16$, separation $\leq 0''.9$) satellite such as Charon simply did not exist prior to about 1965, which may be taken as an approximate earliest bound to the possibility of discovery.

8.3. Geometry (a post–1990 limit)

Several aspects of the geometry of the Pluto–Charon system as seen from our nearly heliocentric (dis)advantage point simultaneously conspire to make the discovery of Charon more likely in the two or three decades prior to the 1990s. We first consider those factors due to the specifics of Pluto's own orbit which have optimized the potential for the discovery of Charon.

As is well-known, Pluto's orbit about the Sun is both highly eccentric ($e = 0.246$) and highly inclined with respect to the ecliptic ($i = 17^\circ.1$). Pluto takes 248 years to complete one circuit about the Sun. The orientation of its orbit ellipse is such that at perihelion Pluto is some 9.2 astronomical units above (to the north of) the ecliptic, and only 29.7 AU from the Sun. (Compare this to its mean distance of 39.5 AU and aphelion distance of 49.3 AU). The planet actually is closer to the Sun than is Neptune for the years 1979–1999, and the first perihelion passage since discovery occurred 1989 September 05 at 2:31 UT (Mink *et al.* 1990). There is no known dynamical reason why Charon's orbital plane should point toward the Sun almost exactly at perihelion. Currently, this alignment must be regarded as purely due to chance, although I find such a configuration to be a bit *too* coincidental, nonetheless.

It is immediately apparent that at perihelion, the Pluto–Charon separation of 19,640 km subtends its largest angular distance, by virtue of its proximity to the

Earth. Additionally, one would naïvely expect Pluto to be at its brightest near perihelion, due to the inverse-square law. (Due to the actual distribution of albedo features on the surface of Pluto, we now know this not to be the case, hence the use of the word "naïvely". See Hardie 1965 and Marcialis 1988*a*.)

A third point of consideration is that, due to the relative orientation of Pluto's orbital ellipse and the Earth's axial obliquity, Pluto reaches its greatest northern declination during the inbound quarter of its 248-year orbit. If one were to make a plot of Pluto's declination at opposition *versus* time, it can be seen that the declination has increased since the discovery in 1930 (when it was in Gemini), culminating at its northernmost value about the year 1946, and has been moving southward ever since. (For simplicity, one may ignore the parallactic effect of the Earth's motion about the Sun, as it amounts to less than $2^\circ\,\mathrm{yr}^{-1}$, and is of only minor consequence to the argument.) Since most of the Earth's major observatories reside in the northern hemisphere (for this century, at least), then studies of Pluto are best conducted when it is at positive declinations. This manifests itself in two different ways. First, the "observing window" (defined here as the amount of time per night that Pluto is high enough in the sky so as to be below 1.5 airmasses) is a strong function of the declination.

Second, for large declinations (up to the colatitude of the observing site, anyway) the altitude of an object above the horizon at meridian passage increases. Thus, one need look through less of the Earth's atmosphere at transit, resulting in greater image stability and therefore plates of superior quality. Taking a concrete example, for an observatory located at approximately 40° North latitude, the maximum observing window in 1946 was $\sim 7^h40^m$, while in 1990 it shall be only $\sim 3^h49^m$. When one folds in the seasonal variation of evening twilight, then the actual usable window in 1990 is further compromised, while the effect in the 1940s is of only slight consequence. This serves only to strengthen the preceding argument.

We now consider the actual orbit of Charon about Pluto, enumerating the various factors which also favor the discovery of Charon prior to the 1990s. Charon orbits Pluto in a circle which is highly inclined to both the ecliptic and Pluto's path about the Sun. In fact, the orbit is oriented such that Charon's motion is almost entirely in the N/S direction; see Figure 1.1.

It should be noted that a low-inclination orbit, *i.e.*, one that is nearly face-on to the observer, is much more conducive to the discovery of a satellite. The face-on geometry ensures that at all times the photocenter of the combined image differs most from its barycenter. Charon's orbit was oriented nearly face-on (much like the Uranian satellite orbits are now positioned) in the 1940s. Unfortunately, the planet was only rarely observed then due to, among other things, the Second World War. Since then the apparent orbit, when projected on the sky plane, has been "closing up," *i.e.*, becoming more elongate with time. At minimum elongations it becomes progressively more difficult to resolve the pair, whose seeing disks overlap even under the best of photographic conditions. During 1988, when the Earth passed through the orbit plane, the bump of Charon could be seen for only two nights per orbit (1 orbit = 6.387245 days), that is, for one night at northern elongation and one at southern—less than one-third of all orbital phases. Even this estimate is optimistic in that it presumes that Pluto be visible from a given observatory near the times such elongations occur, and that the atmosphere then be sufficiently stable so as to permit quality imaging. Rather than a detection rate of 30%, the actual figure is $\sim$10% or less.

So we see that, in order to obtain a reasonable sampling of position angles of Charon with respect to Pluto (a requirement for a good photocentric orbit determination), the temporal constraints on orbital geometry make the discovery *least likely* from about the mid-1980s to the mid-1990s. This latter bound is extended well into the next century when one considers Pluto's declination and the distribution of observatories on the Earth. Although the openness of the orbit may have been less optimal in the 1970s than in previous decades, in a *relative* sense the geometry then was much more conducive to satellite discovery than in the 1980s and 1990s.

8.4. SUMMARY

I have attempted to demonstrate, using several lines of reasoning, that the 1978 discovery of Pluto's only known satellite a scant seven years before the commencement of the mutual events was *not* fortuitous. Rather, the discovery came almost exactly in the middle of a two- to three-decade span of time when its discovery was most favored by the intersection of technological and geometrical factors.

This is in no way intended to dismiss the wonderfully careful and methodical work of Christy, Harrington, and the whole Astrometry Division of the United States Naval Observatory. Rather, the lesson to be learned is that careful and deliberate studies of available datasets, when circumstances are favorable, often will result in important discoveries. Since in most cases one cannot know *a priori* exactly *when* circumstances are favorable, one should always be on one's guard. There is no substitute for care in scientific endeavors; even small observatories can do very big science when properly used.

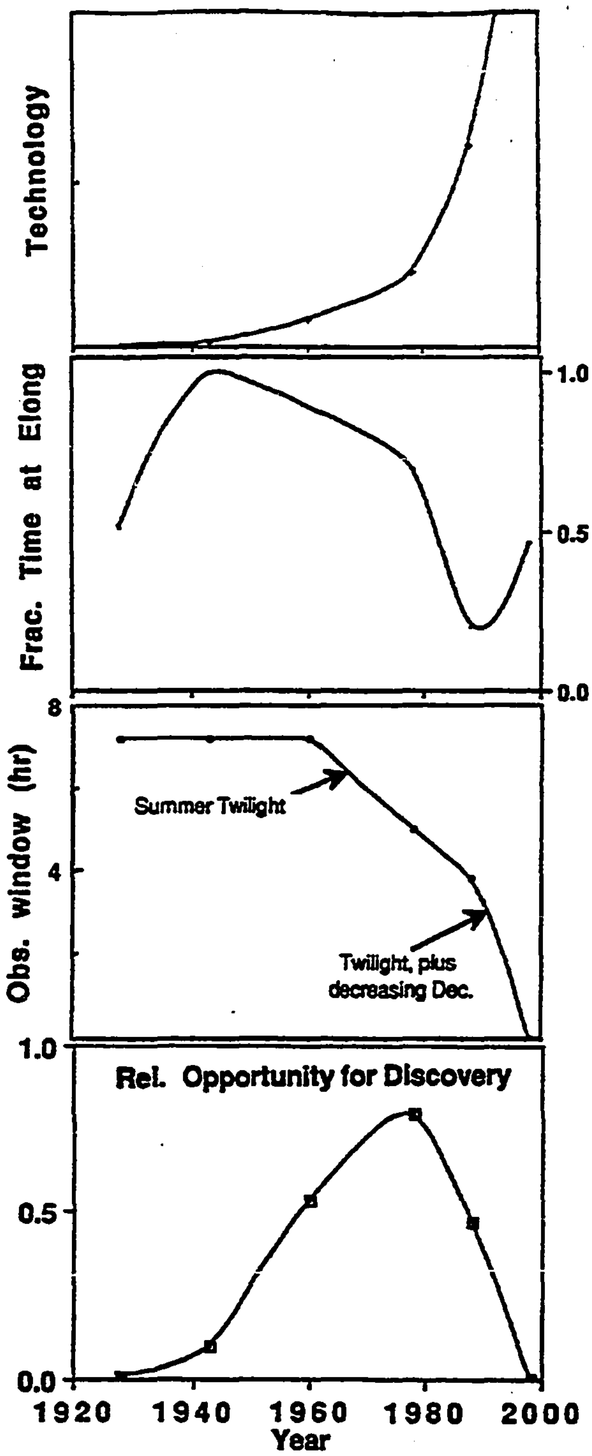

Figure 8.1. (*top to bottom*)
a. Technology increases roughly exponentially with time. This result is simply derived from inversion of the "learning curve," a common engineering concept.
b. As Charon's orbital plane becomes aligned with our line of sight, the satellite spends less time at elongation, the time when its light is separated most readily from Pluto's.
c. Hours per day when Pluto may be observed from an Earth-bound observatory at latitude 40°N.
d. Renormalized product of the four functions yields the relative discovery probability for Charon. The actual discovery was in 1978.

What other lessons may be learned from the discovery circumstances of Charon? Most immediately obvious is that the search for small, close-in satellites of planets and/or asteroids through imaging is most likely to be successful when the orbital planes are "face-on" to the Earth. A notable exception to this idea is that of the planet Saturn; here the bright rings are least objectionable when viewed edge-on. Jupiter's extremely low obliquity dismisses it from consideration. However, when one examines the discovery circumstances for the "classical" satellites of Mars, Uranus, and Neptune, one sees that *essentially all were found during oppositions when their orbits were in a relatively "open" configuration.* Depending on one's point of view, it is unfortunate that the Voyager spacecraft have been so successful in discovering the many satellites of Jupiter, Saturn, Uranus, and Neptune. However, no one should believe that in their brief flybys of the outer giant planets all satellites have been discovered; future groundbased work should be done to search for new members of the solar system. Nature constantly performs experiments in the sky. We have only to be smart enough to understand what these experiments are in order to understand what they mean.

CHAPTER 9

SUMMARY

Comparatively little was known about Pluto and its satellite Charon before the onset of the mutual events in 1985, and much of that was figured out in anticipation of these events. Seen as little more than a point of light from Earth, the system was known to rotate every 6.4 days. The spectral signature of methane was observed, but little was known about its physical state, distribution, and dynamics. Poorly constrained masses and radii made bulk density estimates and interior models little more than educated guesses.

Eclipses and occultations between planet and satellite have proven to be a Rosetta stone with which to unlock many of Pluto's secrets. Individual flux contributions to the meager total sum were determined to demonstrate that the two have different surface albedos.

This experiment was repeated many times, as a function of wavelength, to build up the (distinct) spectra of each body from 0.4–2.5 μm. Pluto's surface is rich in methane frost, while Charon displays a spectrum of water frost, more typical of other (inner) outer satellites.

Atmospheric escape calculations show that the system could have evolved to this state even if both bodies initially had the same methane coating. Pluto may even have accreted a significant amount of Charon's methane in the process. Observation and theory are consistent in understanding this aspect of the system which was unanticipated before the mutual events.

Out-of-eclipse spectrophotometry has been performed to demonstrate that even on the surface of Pluto itself methane distribution is not uniform. At least over one hemisphere, correlation between albedo and composition has been established. Bright terrain appears enriched in surficial methane relative to dark in a manner consistent with the surface albedo model constructed in 1988 for my Master's thesis.

A simple theoretical treatment of the rheology of methane ice has been combined with the most current interior models of Pluto in an effort to determine relaxation times for topographic features. Calculations show that Pluto's figure is expected to be globally hydrostatic, and that features with horizontal scales much larger than a few to several tens of kilometers cannot have persisted over the age of the solar system. In addition to compositional differences, the surfaces of planet and satellite are expected to have disparate geological expressions, such as crater size-frequency distributions. A more complicated visco-elastic treatment of the problem certainly is justified to see if these conclusions are robust.

Astrometric observations of the Pluto–Charon photocenter have been obtained and reduced. These measurements are useful for the constant chores of refining Pluto's heliocentric orbit and predicting potential stellar occultations by planet and satellite.

Finally, geometrical, technological, and historical contributions have been examined to demonstrate that the discovery of Charon a scant few percent of an orbit before the mutual events ensued probably was not coincidental. Rather, the discovery came at a time when these contributors actually maximized the discovery probability. A far cry from archeoastronomy, but a small contribution to the history of the field, nevertheless.

In the course of my graduate study, Pluto and Charon have become individual worlds, distinct from the other bodies in the solar system as well each other. Although individuals, their relationship probably is more symbiotic than any other planet-satellite pair in the solar system as a result of their close proximity. It is unique in being the only planetary system whose barycenter lies *outside* the body of the primary. Study of one body oftentimes is thwarted by the presence of the other, but a great wealth of information has been realized due to their close association.

I look forward to the many new things the Hubble Space Telescope undoubtedly will reveal about this binary planet as it recedes from perihelion. Yet neither the HST nor any space-based telescope even dreamed of now can compete with synoptic observations of the system from the ground, from scheduling, aperture, and orbital considerations. So much remains to be done.

In many respects, Pluto and Charon form a unique and very special laboratory where nature constantly conducts some pretty interesting experiments. The Pluto–Charon system presents a continual challenge for me to figure out just what these experiments are, and provides an excellent example of the interdisciplinary nature of astronomy and the planetary sciences.

APPENDIX A: END NOTES

Most of the chapters in this dissertation have been or will be published as separate investigations in the refereed literature. For those chapters dealing with observations made at facility telescopes, several institution require (and deserve) specific credit lines to be attached to any publication derived from observations made there. The purpose of this Appendix is to comply with these regulations, in a manner which is acceptable to the rigid regulations of the Graduate College in describing original research. By chapter, these are the appropriate credit lines:

The surface composition of Charon: tentative identification of water ice. We thank the staff of the Multiple Mirror Telescope for their extra efforts in accommodating a one-night observing run and the 12 secondary mirror changes it entailed. This work was partially supported by NASA grants NGT–50048 and NSG–7114, and by the NSF. Observations reported in this report were obtained at the Multiple Mirror Telescope Observatory, a joint facility of the University of Arizona and the Smithsonian Institution.

Escape of methane from Charon. This chapter was the Appendix to a term paper for the course, "Ices in the Solar System," taught by J.I. Lunine at the University of Arizona in the spring of 1987. It was submitted two days before Dr. Lunine was asked to referee a very similar paper by Trafton, Stern, and Gladstone (1988). The results were nearly identical, with most of the small differences attributable to adopted values of numerical constants. In the chapter, values for various parameters in the Pluto–Charon system have been updated to their most current values. The author would like to thank the brewers of America for consumables used in the calculations. Also thanks to my fine officemates, Paul Geissler and Ellen Bus for assistance in the use of the plotting package used for most of the graphics in this dissertation.

CVF spectrophotometry of Pluto: correlation of composition with albedo. Larry Lebofsky and Robert Marcialis were visiting astronomers at the Infrared Telescope Facility, which is operated by the University of Hawaii under contract to NASA. The paper has been submitted to *Icarus* with only minor editorial changes. This work was partially supported by NASA grants NGT–50048 and NSG–7114. Many thanks to Charles Kaminski, William Golisch, and David Griep, who as always do a fine job of piloting the IRTF during the nights of observations. Along with Dr. Mike Gaffey, they provided invaluable assistance in bringing me up to speed on the use of the instruments. Their friendship is appreciated.

The albedos of Pluto and Charon: wavelength dependence. After my coauthors respond with (hopefully constructive) comments, this chapter will be submitted to *Icarus*. MMTO observations reported in this paper were obtained (by RLM, GHR, LAL) at the Multiple Mirror Telescope Observatory, a joint facility of the University of Arizona and the Smithsonian Institution. ET was a guest investigator at Kitt Peak National Observatory, operated by Associated Universities for Research in Astronomy, Inc. The authors acknowledge support from NASA grants NGT–50048, NGT–50047, NSG–7070, and NSG–7114, and from the NSF. EFT's portion of the research described in this paper was carried out at the Jet Propulsion Laboratory, California Institute of Technology, under contract with the National Aeronautics and Space Administration.

Astrometric observations of Pluto: 1965–1981. The authors would like to thank Drs. P.M. Routly and R.S. Harrington for the hospitality and entertainment they provided during our stay at the U.S. Naval Observatory in Washington.

We will always remember with fondness the late Dr. Bob Hardie, whose grant funded the trip to the USNO. Non-thanks to E. Levy, who made me pay the page charge out of my own pocket.

Topographic relaxation on ice-covered worlds: application to Pluto. This chapter started out as the term paper for the course, "Planetary Surfaces," taught by H.J. Melosh at the University of Arizona in the spring of 1985. In addition to being a fine researcher in his field, Jay is clearly the finest teacher at the Lunar & Planetary Laboratory. My promise to him that the work will be submitted for publication has been kept. Recently, some experimental data on the rheology of methane has been published, and should be incorporated into the final version of the paper. Steve Croft and Paul Geissler provided useful information in several conversations regarding this work.

The discovery of Charon: happy accident or timely find? appeared in the *Journal of the British Astronomical Association* after being rejected by the *Journal for the History of Astronomy* as being "too technical." Thanks to an anonymous referee and Dr. J. Mitton for their efforts. Dr. Clyde Tombaugh's entertaining lecture recounting his discovery of Pluto was the initial inspiration for this investigation. This work was supported by NASA grants NGT–50048 and NSG–7114, and was given as an invited talk at the 20th meeting of the American Astronomical Society's Division of Planetary Sciences (Marcialis 1988*c*).

Although time constraints have precluded inclusion of visual (Johnson B and Cousins R) photometry of the Pluto–Charon mutual events, I wish to thank Drs. D. Hunten and W. Hubbard for their technical assistance with the photometers used. Thanks to the numerous people who have served on the University of Arizona Observatories Telescope Allocation Committee for the many nights granted, and to

Marcia Rieke for scheduling these rather inconvenient one-night stints. Appreciation is also extended to Dennis Means and John Waack for operating the Steward Observatory Kitt Peak 90″ on the numerous nights data were obtained, and the equal number of nights when the weather was aphotometric. Thanks to Russ Rymer of *The Sciences* for documenting one of those observing runs; I wish the weather had cooperated.

Many useful discussions and collaborations with scientists both at the Lunar & Planetary Laboratory and elsewhere have resulted in other projects which unfortunately could not be included as part of this dissertation. In particular, it has been a pleasure to work with Rick Greenberg on our thermal modelling of Miranda, and also on the chapter "Miranda" for the U. of A. Press Series book *Uranus*. Good luck with playing advisor to my housemates, Mike Nolan and Bill Bottke. You'll need it.

Jonathan Lunine, Steven Croft, Wiesław Wiśniewski, Mark Sykes, John Spencer, Nick Schneider, Gordy Bjoraker, Dave Grinspoon, John Stansberry, Steve Larson, Don Davis, Stu Weidenschilling, Bill Hartmann, Bob Millis, Irwin Shapiro, Joel Eaton, Jim and Alan Sowell, John Wilson, Gene Eplee, Pat Hartigan, Dale Cruikshank, and Ed Tedesco have, through discussions and advice, contributed in some form to my research and development as a scientist over the past decade. Thanks to J.R. Jokipii for assistance in incorporating graphics into this document.

Total disinformation is nevertheless useful for learning about something, and there are those who have supplied their fair share over the years. To them, I offer my non-thanks. Some of you don't not know who you are; however, I won't supply your names anyway.

LPL could not function without all the great support staff it has. My hat is off to the many secretaries, administrators, machinists, budget jockeys, and library staff who make the Lab such a fine research environment.

Most will agree that the time one writes a thesis or dissertation is a close approximation to a stint in Hell. (Now that I think of it, that *is* a reasonable analogy when the topic of research is Pluto ...) During such times, there is always one individual who takes the outsider's point of view. They constantly pester the author with annoying questions like, "Isn't a 30-hour stint in front of the terminal long enough?" and, "When was the last time you ate?" The author usually makes lame comments like, "NO! ... What day is it? ... What do you mean I'm cut? I don't have time to bleed." This time around, that pestering person was Marcia (no, it's pronounced *Már sya*) Nelson. Thanks for dragging me out for the occasional snack. (By the way, I wouldn't have listened to her had she not just gone through the same ordeal.) I wish ... our time of overlap at the Looney Lab was longer.

In addition to being a swell Joes and goofy characters in their own right, Bill "Gramps" Merline and Marcus "Marconi" Perry deserve mention. Marcus was the first character I laid eyebones on upon my arrival at the Lab, and has been a friend ever since. Bill, get it in gear and write that stupid dissertation. In a burning building, the best advice is to "get out of the house!" What can I say to Dr. Al Schultz, except, "quit slamming the †*# & § ¿ @!↗ • ⌒ ⋆ doors!"

Good luck to Lisa McFarlane, Will Grundy, Shelly Pope, Kent Wells, Erik Asphaug, Valerie Hillgren, Doyle Hall, Ann Sprague, and Tom Jones, our newest astronaut. And to "Midnight" Mark Marley who beat me to Ph.D. by exactly 1 week. (I'd have won if *you* wrote the formatting macro...) Grace "Graciélaga"

Wolf is referred to the advice to Gramps. Data collection and reductions are time-consuming, often thankless, but always unique, contributions an individual can make to his chosen field. *Someone* has to keep the theoreticians honest. But get 'em, do 'em, and get 'em out so they can be shared by everyone.

REFERENCES

ANDERSSON, L.E. (1978) Eclipse phenomena of Pluto and its satellite. *Bull. Amer. Astron. Soc.* **10**, 586 (Abstract).

BATCHELOR, G.K. (1967) *An Introduction to Fluid Mechanics.* Cambridge University Press, London, p. 174.

BEATTY, J.K. (1985) Pluto and Charon: the dance begins. *Sky and Tel.* **69**, 501–502.

BELETIC, J.W., GOODY, R.M., AND THOLEN, D.J. (1989) Orbital elements of Charon from speckle interferometry. *Icarus* **79**, 38–46.

BINZEL, R.P. AND MULHOLLAND, J.D. (1983) Photometry of Pluto during the 1982 opposition. *Astron. Jour.* **88**, 222–225.

BINZEL, R.P. AND MULHOLLAND, J.D. (1984) Photometry of Pluto during the 1983 opposition: A new determination of the phase coefficient. *Astron. Jour.* **89**, 1759–1761.

BINZEL, R.P., THOLEN, D.J., TEDESCO, E.F., BURATTI, B.J., AND NELSON, R.M. (1985) The detection of eclipses in the Pluto–Charon system. *Science* **228**, 1193–1195.

BINZEL, R.P. (1988) Hemispherical color differences on Pluto and Charon. *Science* **241**, 1070–1071.

BONNEAU, D. AND FOY, R. (1980) *Interférométrie au 3.60 m CFH. I. Résolution de système Pluto–Charon.* (Speckle interferometry with the CFHT 3.60 m I. Resolution of the Pluto–Charon system). *Astron. Astrophys.* **92**, L1–L4.

BROWN, JR., G.N. AND ZIEGLER, W.T., in *Advances in Cryogenics Engineering*, K.D. Timmerhaus and H.A. Snyder, eds. (Plenum Press, New York, 1979), vol. **25**, pp. 662–669.

BUIE, M.W. (1984) *Lightcurve CCD spectrophotometry of Pluto.* Ph.D. dissertation, University of Arizona, Tucson.

BUIE, M.W. AND FINK, U. (1987) Methane absorption variations in the spectrum of Pluto. *Icarus* **70**, 483–498.

BUIE, M.W., CRUIKSHANK, D.P., LEBOFSKY, L.A., AND TEDESCO, E.F. (1987) Water frost on Charon. *Nature* **329**, 522–523.

BUIE, M.W., LEBOFSKY, L.A., TEDESCO, E.F., AND CRUIKSHANK, D.P. (1989) Methane map for Pluto based on mutual events. *Bull. Amer. Astron. Soc.* **21**, 985 (Abstract).

BUIE, M.W. AND THOLEN, D.J. (1989) The surface albedo distribution of Pluto. *Icarus* **79**, 23–37.

CAMPINS, H., RIEKE, G.H., AND LEBOFSKY, M.J. (1985) Absolute calibration of photometry at 1 through 5 μm. *Astron. Jour.* **90**, 896–899.

CHENG, A.F., HAFF, P.K., JOHNSON, R.E., AND LANZEROTTI, L.J. (1986) "Interactions of planetary magnetospheres with icy satellite surfaces," in *Satellites* (J.A. Burns and M.S. Matthews, eds., University of Arizona Press, Tucson), pp. 403–436.

CHENG, A.F. AND JOHNSON, R.E. (1989) "Effects of magnetospheric interactions on origin and evolution of atmospheres," in *Origin and evolution of planetary and satellite atmospheres* (S.K. Atreya, J.B. Pollack, and M.S. Matthews, eds., University of Arizona Press, Tucson), pp. 682–722.

CHRISTY, J.W. AND HARRINGTON, R.H. (1978) The satellite of Pluto. *Astron. Jour.* **83**, 1005–1008.

CONSOLMAGNO, G.J. AND LEWIS, J.S. (1978) The evolution of icy satellite interiors and surfaces. *Icarus* **34**, 280–293.

CRUIKSHANK, D.P., PILCHER, C.B., AND MORRISON, D. (1976) Pluto: Evidence for methane frost. *Science* **194**, 835–837.

CRUIKSHANK, D.P., PILCHER, C.B., AND MORRISON, D. (1977) Identification of a new class of satellites in the outer solar system. *Astrophys. Jour.* **217**, 1006–1010.

CRUIKSHANK, D.P. AND SILVAGGIO, P.M. (1980) The surface and atmosphere of Pluto. *Icarus* **41**, 96–102.

CRUIKSHANK, D.P. AND BROWN, R.H. (1986) "Satellites of Uranus and Neptune, and the Pluto–Charon system," in *Satellites* (J.A. Burns and M.S. Matthews, eds., University of Arizona Press, Tucson), pp. 836–873.

CRUIKSHANK, D.P., BROWN, R.H., GIVER, L.P., AND TOKUNAGA, A.T. (1989) Triton: do we see the surface? *Science* **245**, 283–286.

DODD, R.J. (1972) Precise stellar positions using GALAXY-machine measurements of a Schmidt plate. *Astron. Jour.* **77**, 306–311.

DUNBAR, R.S. AND TEDESCO, E.F. (1980) Modeling Pluto–Charon mutual eclipse events I. First order models. *Astron. Jour.* **92**, 1201–1209.

ELLIOT, J.L., DUNHAM, E.W., BOSH, A.S., SLIVAN, S.M., YOUNG, L.A., WASSERMAN, L.H., AND MILLIS, R.L. (1989) Pluto's atmosphere. *Icarus* **77**, 148–170.

ELLSWORTH, K. AND SCHUBERT, G. (1983) Saturn's icy satellites: thermal and structural models. *Icarus* **54**, 490–510.

FINK, U., SMITH, B.A., BENNER, D.C., JOHNSON, J.R., AND REITSEMA, H.J. (1980) Detection of a CH_4 atmosphere on Pluto. *Icarus* **44**, 62–71.

FINK, U. AND SILL, G.T. (1982) "The infrared spectral properties of frozen volatiles," in *Comets* (L. Wilkening, ed. U. of Arizona Press, Tucson), pp. 164–202.

FINK, U. AND LARSON, H.P. (1975) Temperature dependence of the water-ice spectrum between 1 and 4 μms: application to Europa, Ganymede, and Saturn's rings. *Icarus* **24**, 411–420.

FINK, U. AND DISANTI, M.A. (1988) The separate spectra of Pluto and its satellite Charon. *Astron. Jour.* **95**, 229–236.

HARDIE, R.H. (1965) A re-examination of the light variation of Pluto. *Astron. Jour.* **70**, 140.

HARDIE, R.H., MARCIALIS, R.L., WILSON, J.W., AND FURMAN, W.R. (1984) Astrometric observations of Pluto from 1965–1981. *Astron. Jour.* **90**, 2643.

HARDORP, J. (1980) The Sun among stars III. Energy distributions of 16 Northern G-type stars and the solar flux calibration. *Astron. Astrophys.* **91**, 221–262.

Harrington, R.S. and Mintz, B.F. (1972) "Positions of bright minor planets," in *Publ. USNO XXIII, Part 3* (U.S. Naval Observatory, Washington, D.C.), p. 7.

HASKELL, N.A. (1935) The motion of a viscous fluid under a surface load. *Physics* **6**, 265–269.

HASKELL, N.A. (1936) The motion of a viscous fluid under a surface load. *Physics* **7**, 56–61.

HUGHES, T.J. (1976) The theory of thermal convection in polar ice sheets. *Jour. Glaciology* **16**, 41–71.

HUBBARD, W.B., HUNTEN, D.M., DIETERS, S.W., HILL, K.M., AND WATSON, R.D. (1988) Occultation evidence for an atmosphere on Pluto. *Nature* **336**, 452–454.

HUBBARD, W.B., YELLE, R.V., AND LUNINE, J.I. (1990) Nonisothermal Pluto atmosphere models. *Icarus*, in press.

HUNTEN, D.M. (1973) The escape of light gases from planetary atmospheres. *Jour. Atmos. Sci.* **30**, 1481–1494.

HUNTEN, D.M. AND WATSON, A.J. (1982) Stability of Pluto's atmosphere. *Icarus* **51**, 665–667.

HUNTEN, D.M., DONAHUE, T.M., WALKER, J.C.G., AND KASTING, J.F. (1989) "Escape of atmospheres and loss of water," in *Origin and evolution of planetary and satellite atmospheres* (S.K. Atreya, J.B. Pollack and M.S. Matthews, eds., University of Arizona Press, Tucson), pp. 386–422.

JEANS, J.H. (1925) *The dynamical theory of gases.* (Cambridge University Press), Chapter 15.

JOHNSON, R.E. (1989) Effect of irradiation on the surface of Pluto. *Geophys. Res. Letters* **16**, 1233–1236.

KUIPER, G.P. (1961) "Limits of Completeness," in *Planets and Satellites* (G.P. Kuiper and B.M. Middlehurst, eds., University of Chicago Press, Chicago), Chapter 18.

LEBOFSKY, L.A., RIEKE, G.H., AND LEBOFSKY, M.J. (1979) Surface composition of Pluto. *Icarus* **37**, 554–558.

LUNINE, J.I., ATREYA, S.K., AND POLLACK, J.B. (1986) "Present state and chemical evolution of the atmospheres of Titan, Triton, and Pluto," in *Origin and evolution of planetary and satellite atmospheres* (S.K. Atreya, J.B. Pollack, and M.S. Matthews, eds., University of Arizona Press, Tucson), pp. 605–665.

LUPO, M.J. AND LEWIS, J.S. (1980*a*) Mass–radius relationships and constraints on the composition of Pluto. *Icarus* **42**, 29–34.

LUPO, M.J. AND LEWIS, J.S. (1980*b*) Mass–radius relationships and constraints on the composition of Pluto, II. *Icarus* **44**, 41–42.

MARCIALIS, R.L. (1983) *A two spot model for the surface of Pluto.* Master's Thesis, Vanderbilt University, Nashville, Tennessee.

MARCIALIS, R.L. (1984) A two spot model for the surface of Pluto. *Bull. Amer. Astron. Soc.* **16**, 651 (Abstract).

MARCIALIS, R.L. (1985) Topographic relaxation on ice–covered worlds: application to Pluto. *Bull. Amer. Astron. Soc.* **17**, 715 (Abstract).

MARCIALIS, R.L., RIEKE, G.R., AND LEBOFSKY, L.A. (1987) The surface composition of Charon: tentative identification of water ice. *Science* **237**, 1349–1351.

MARCIALIS, R.L. (1988*a*) A two–spot albedo model for the surface of Pluto. *Astron. Jour.* **95**, 941–947.

MARCIALIS, R.L. (1988*b*) Spotting Pluto. (Letter to editor). *Sky and Tel.* **75**, 6.

MARCIALIS, R.L. (1988*c*) The discovery of Charon: happy accident or timely find? *Bull. Amer. Astron. Soc.* **20**, 840 (Abstract).

MARCIALIS, R.L. (1988*d*) The discovery of Charon: happy accident or timely find? *Jour. Brit. Astron. Soc.* **99**, 27–29.

MARCIALIS, R.L. (1989) Topographic relaxation on ice–covered worlds: application to Pluto II. *Eos* **70**, 386.

MARCIALIS, R.L. (1989) Topographic relaxation on ice–covered worlds: application to Pluto. Submitted to *Geophys. Res. Letters*.

MARCIALIS, R.L., AND LEBOFSKY, L.A. (1990) CVF spectrophotometry of Pluto: correlation of composition and albedo. Submitted to *Icarus.*

MCKINNON, W.B. AND MUELLER, S. (1988) Pluto's structure and composition suggest origin in the solar, not a planetary, nebula. *Nature* **335**, 240–243.

MINK, D., KLEMOLA, A.R., AND BUIE, M.W. (1990) Occultations by Pluto and Charon: 1990–1999. Submitted to *Astron. Jour.*

MULHOLLAND, J.D. AND GUSTAFSON, B.Å.S. (1987) Pluto eclipses of and by Charon must be unequal. *Astron. Astrophys.* **171**, L5–L7.

PARMENTIER, E.M. AND HEAD, J.W. (1979) Internal processes affecting surfaces of low-density satellites: Ganymede and Callisto. *Jour. Geophys. Res.* **84**, 6263–6276.

PARMENTIER, E.M., ALLISON, M.L., CINTALA, M.J., AND HEAD, J.W. (1980) Viscous degradation of impact craters on icy satellite surfaces. *Lunar and Planetary Science* **XI**, 857–859.

PARMENTIER, E.M. AND HEAD, J.W. (1981) Viscous relaxation of impact craters on icy planetary surfaces: determination of viscosity variation with depth *Icarus* **47**, 100–111.

POIRER, J.P. (1982) Rheology of ices: a key to the tectonics of the ice moons of Jupiter and Saturn. *Nature* **299**, 683–688.

RIDDLE, R.K. AND WORLEY, C.E. (1966) Applications of automatic measuring machines to astrometry. *Astron. Jour.* **71**, 868.

SAWYER, S.R. (1986) *Time resolved spectrophotometry of Pluto.* Thesis, University of Texas at Austin.

SAWYER, S.R., BARKER, E.S., COCHRAN, A.L., AND COCHRAN, W.D. (1987) CCD spectrophotometry of Pluto–Charon mutual events. *Bull. Amer. Astron. Soc.* **19**, 859 (Abstract).

SAWYER, S.R. (1989) Reflectance spectroscopy of the surface and atmosphere of Pluto–Charon. *Bull. Amer. Astron. Soc.* **21**, 986 (Abstract).

SCHUBERT, G., STEVENSON, D.J., AND ELLSWORTH, K. (1981) Internal structures of the Galilean satellites. *Icarus* **47**, 46–59.

SCOTT, R.F. (1967) Viscous flow of craters. *Icarus* **7**, 139–148.

SEYFERT, C.K. (1956) The Baker-Schmidt telescope of the Arthur J. Dyer Observatory. *Mitt. Astron. Ges.* **1955**, 77.

SIMONELLI, D.P., POLLACK, J.B, MCKAY, C.P., REYNOLDS, R.T., AND SUMMERS, A.L. (1989) The carbon budget in the outer solar nebula. *Icarus* **82**, 1–36.

SIMONELLI, D.P. AND REYNOLDS, R.T. (1989) The interiors of Pluto and Charon: structure, composition, and implications. *Geophys. Res. Letters* **16**, 1205–1212.

SMITH, B.A., SODERBLOM, L.A., BANFIELD, D., BARNET, C., BASILEVSKY, A.T., BEEBE, R.F., BOLLINGER, K., BOYCE, J.M., BRAHIC, A., BRIGGS, G.A., BROWN, R.H., CHYBA, C., COLLINS, S.A., COLVIN, T., COOK II, A.F., CRISP, D., CROFT, S.K., CRUIKSHANK, D., CUZZI, J.N., DANIELSON, G.E., DAVIES, M.E., DEJONG, E., DONES, L., GODFREY, D., GOGUEN, J., GRENIER, I., HAEMMERLE, V.R., HAMMEL, H., HANSEN, C.J., HELFENSTEIN, C.P., HOWELL, C., HUNT, G.E., INGERSOLL, A.P., JOHNSON, T.V., KARGEL, J., KIRK, R., HUEHN, D.I., LIMAYE, S., MASURSKY, H., MCEWEN, A., MORRISON, D., OWEN, T., OWEN, W., POLLACK, J.B., PORCO, C.C., RAGES, K., ROGERS, P., RUDY, D., SAGAN, C., SCHWARTZ, J., SHOEMAKER, E.M., SHOWALTER, M., SICARDY, B., SIMONELLI, D., SPENCER, J., SROMOVSKY, L.A., STOKER, C., STROM, R.G., SUOMI, V.E., SYNOTT, S.P., TERRILE, R.J., THOMAS, P., THOMPSON, W.R., VERBISCER, A., AND VEVERKA, J. (1989) Voyager 2 at Neptune: imaging science results. *Science* **246**, 1422–1449.

SOIFER, B.T., NEUGEBAUER, G., AND MATTHEWS, K. (1980) The 1.5–2.5 micron spectrum of Pluto. *Astrophys. Jour.* **85**, 166–167.

SPITZER, JR., L. (1952) "The terrestrial atmosphere above 300 kilometers," in *The atmospheres of the Earth and the planets* (G.P. Kuiper, ed. University of Chicago Press, Chicago), pp. 211–247.

STANSBERRY, J.A., LUNINE, J.I., AND TOMASKO, M.L. (1989) Upper limits on possible photochemical hazes on Pluto. *Jour. Geophys. Res.* **16**, 1221–1224.

STERN, S.A. AND TRAFTON, L.M. (1984) Constraints on bulk composition, seasonal variation, and global dynamics of Pluto's atmosphere. *Icarus* **57**, 231–240.

STERN, S.A., TRAFTON, L.A., AND GLADSTONE, G.R. (1988) Why is Pluto bright? Implications of the albedo and lightcurve behavior of Pluto. *Icarus* **75**, 485–498.

STRAND, K.Å. (1966) New automatic measuring machine. *Astron. Jour.* **71**, 873.

STRAND, K.Å. (1971) The 61-inch astrometric reflector. *Pub. U.S.N.O., Second Series* **Vol. XX**, Part I.

THOLEN, D.J. AND TEDESCO, E.F. (1984) Photometry of the Pluto/Charon system. *Bull. Amer. Astron. Soc.* **16**, 923 (Abstract).

THOLEN, D.J. (1987) The orbit of Pluto's satellite. *Astron. Jour.* **90**, 2353–2359.

THOLEN, D.J., BUIE, M.W., BINZEL, R.P., AND FRUEH, M.L. (1987*a*) Improved orbital and physical parameters for the Pluto–Charon system. *Science* **237**, 512–514.

THOLEN, D.J., BUIE, M.W., AND SWIFT, C.E. (1987*b*) Circumstances for Pluto–Charon mutual events in 1987. *Astron. Jour.* **93**, 244–248.

THOLEN, D.J. AND BUIE, M.W. (1988) Circumstances for Pluto–Charon mutual events in 1989. *Astron. Jour.* **96**, 1977–1982.

THOLEN, D.J. (1989) Results from five years of Pluto–Charon mutual event observations. *Eos* **70**, 385.

THOLEN, D.J. AND BUIE, M.W. (1989) Further analysis of Pluto–Charon mutual event observations — 1989. *Bull. Amer. Astron. Soc.* **21**, 981–982 (Abstract).

TRAFTON, L. (1980) Does Pluto have a substantial atmosphere? *Icarus* **44**, 53–61.

TRAFTON, L.M., STERN, S.A., AND GLADSTONE, G.R. (1988) The Pluto–Charon system: escape of Charon's primordial atmosphere. *Icarus* **74**, 108–120.

VAN FLANDERN, T.C., KAPLAN, G.H., PULKKINEN, K.F., SANTORO, E.J., AND SEIDLEMANN, P.K. (1981) The period of Charon, as derived from the observed barycentric motion of Pluto. *Bull. Amer. Astron. Soc.* **13**, 573 (Abstract).

WALKER, M.F., AND HARDIE, R.H. (1955) A photometric determination of the rotational period of Pluto. *Pub. Astron. Soc. Pacific* **67**, 224–231.

WALKER, A.R. (1980) An occultation by Charon. *Mon. Not. Roy. Astron. Soc.* **192**, 47P–50P.

WATSON, A.J., DONAHUE, T.M., AND WALKER, J.C.G. (1981) The dynamics of a rapidly escaping atmosphere: application to the evolution of Earth and Venus. *Icarus* **48**, 150–166.

WHIPPLE, A.R., TRAFTON, L.M., AND STERN, S.A. (1989) A gravitational restricted three-body model of Pluto's upper atmosphere. *Bull. Amer. Astron. Soc.* **21**, 982 (Abstract).

"MMTO Visiting Astronomer Information," *Multiple Mirror Telescope Observatory Technical Report No. 13*, (University of Arizona–Smithsonian Institution, Tucson, December, 1986), pp. 11–12.